UNIVERSITÀ DI PISA

DIPARTIMENTO DI INGEGNERIA DELL'INFORMAZIONE

ELETTRONICA, INFORMATICA, TELECOMUNICAZIONI

ANALYSIS OF THE INFLUENCE OF NON-STATIONARITY OF SEA CLUTTER ON COVARIANCE MATRIX ESTIMATION AND ITS IMPACT ON CFAR DETECTION

Fulvio Gini, Maria S. Greco

and

Muralidhar Rangaswamy*

collaborating engineer from the Air Force Research Laboratory

Pisa, November 2007

REPORT DOCUMENTATION PAGE

Form Approved OMB No. 0704-0188

1. REPORT DATE *(DD-MM-YYYY)* 20-12-2007	2. REPORT TYPE Final Report	3. DATES COVERED *(From – To)* 1 March 2006 - 30-Sep-08

4. TITLE AND SUBTITLE	5a. CONTRACT NUMBER
'Analysis of the Influence of Non-Stationary of Sea Clutter on Covariance Matrix Estimation and its Impact on CFAR Detection	FA8655-06-1-3010
	5b. GRANT NUMBER
	5c. PROGRAM ELEMENT NUMBER

6. AUTHOR(S)	5d. PROJECT NUMBER
Professor Fulvio Gini	
	5d. TASK NUMBER
	5e. WORK UNIT NUMBER

7. PERFORMING ORGANIZATION NAME(S) AND ADDRESS(ES)	8. PERFORMING ORGANIZATION REPORT NUMBER
University of Pisa Via Caruso, 14 Pisa 56122 Italy	N/A

9. SPONSORING/MONITORING AGENCY NAME(S) AND ADDRESS(ES)	10. SPONSOR/MONITOR'S ACRONYM(S)
EOARD Unit 4515 BOX 14 APO AE 09421	
	11. SPONSOR/MONITOR'S REPORT NUMBER(S) Grant 06-3010

12. DISTRIBUTION/AVAILABILITY STATEMENT

Approved for public release; distribution is unlimited.

13. SUPPLEMENTARY NOTES

14. ABSTRACT

This report results from a contract tasking University of Pisa as follows: The research is divided in two phases. In the first phase, we consider modeling and estimating the characteristic parameters of high resolution non-Gaussian sea clutter. We will investigate specifically non-stationarity and possible non-Gaussianity of the clutter on long period of time, by applying nonhomogeneity tests and spectral analysis to highlight the temporal changes of the clutter process. The analyses of high resolution clutter will be performed by processing complex clutter data collected in November 1993 and in winter 1998 with the high resolution IPIX radar, provided by McMaster University, at a range resolution of 60 m, 30 m, 15 m, 9 m, and 3 m, in like- (HH-VV) and crosspolarizations (HV-VH)

An accurate characterization of the high resolution radar clutter allows a more adequate design of the radar detector of targets. This detector needs to be adaptive to the data and should have the ability to comply with the non-homogeneous nature of the clutter interference. This aspect of the problem will be discussed in the second phase of this study. A detailed analysis of the impact of the nonstationarity of the clutter will be performed first analytically (where possible) and by means of simulations; then we will use the real recorded data to feed adaptive detectors, designed for stationary Gaussian and non-Gaussian clutter, and we will compare theoretical and simulated performance with real data performance..

15. SUBJECT TERMS

EOARD, Electromagnetics, radar, Antennas

16. SECURITY CLASSIFICATION OF:			17. LIMITATION OF ABSTRACT UL	18, NUMBER OF PAGES	19a. NAME OF RESPONSIBLE PERSON GEORGE W YORK, Lt Col, USAF
a. REPORT UNCLAS	b. ABSTRACT UNCLAS	c. THIS PAGE UNCLAS		48	19b. TELEPHONE NUMBER *(Include area code)* +44 (0)1895 616163

Standard Form 298 (Rev. 8/98)
 Prescribed by ANSI Std. Z39-18

Abstract

In this report we describe our analysis of the influence of sea clutter non stationarity on the clutter covariance matrix estimation and its impact on the CFAR property of the normalized adaptive matched filter (NAMF). Three estimators have been considered in the analysis, i.e. the sample covariance matrix (SCM), the normalized sample covariance matrix (NSCM), and the fixed point (PF) estimators. The impact of non-stationarity, that emerges in the statistical analysis of the HH and VV polarized data, is measured in terms of differences between NAMF nominal probability of false alarm (P_{FA}) and probability of detection (P_D), and estimated ones measured by processing real clutter data recorded by the IPIX radar.

CONTENTS

1. Introduction

To mitigate the deleterious effects of clutter and jammer, modern radars have adopted adaptive processing techniques such as constant false alarm rate (CFAR) detectors, adaptive arrays, and space time adaptive processing (STAP) (see for instance [Kel86], [Him98], [Kra05], [Mel96], [Mel97], [Ran04], [Ric96], [War94], and reference therein). In a typical adaptive radar system, the disturbance covariance matrix is estimated using secondary data, namely returns from range cells spatially close to the cell under test (CUT) and sharing the same spectral properties [Kel86]. In practice, these techniques are very restrictive because they require the environment to "remain stationary and homogenous" during adaptation, which is not always the case. In fact, the secondary data are often contaminated by interfering targets, large discrete and spiky clutter and other outliers of different types making them non-homogenous. The deleterious impact of this kind of non-homogeneity on the detection performances is widely reported in the literature and several solutions have been proposed [Ger02], [Ran05]. However, another kind of non-homogeneity is caused by the non-stationary nature of the clutter which also has a harmful effect on the radar performances. Recent works on real data revealed that the sea clutter is a non stationary process [Hay02], [Gre04]. Here, we propose to analyze this effect and its impact on CFAR behavior of one of the mostly used adaptive radar detector, the Normalized Adaptive Matched Filter (NAMF).

2. Background

The problem of radar detection in non Gaussian sea clutter has received considerable attention in recent past and currently, a substantial bulk of work is available in the open literature about this topic [Con94], [Con95], [Gin97]. Experimental data as well as physical and theoretical arguments indicate that the clutter can generally be modeled as a compound-Gaussian process and also show that a satisfactory fit of the clutter amplitude probability density function (apdf) at low grazing angles can be achieved through families of distributions containing a shape parameter in addition to the scale one [Far97], [Con02b], [Gre07]. Among these, the most commonly adopted are the Weibull and K distributions, that are particular cases of the compound-Gaussian family.

Conventional radar detectors, namely those designed to detect targets embedded in Gaussian clutter, show considerable performance degradation in the presence of impulsive noise, even in the case of perfect knowledge of the clutter distribution parameters [Con94]. Optimized detection structures have been proposed and assessed with reference to coherent pulse trains embedded in Weibull or K distributed clutter with known spectral properties. However, implementation of these detection structures requires knowledge of clutter statistics up to the relevant distribution parameters, which is clearly unrealistic in practical situations. Thus, one is interested in canonical receivers, namely, decision statistics functionally independent of the clutter distribution parameters (under the noise-only hypothesis) and whose detection threshold is itself independent of the clutter statistics. A first step towards this task is the receiver introduced in [Con95], called the normalized matched filter (NMF) which ensures the CFAR property with respect to clutter distribution (in the family of compound-Gaussian models). This detector has also been derived assuming Gaussian disturbance; Kraut *et alii* in [Kra05] demonstrated that it is the GLRT and Uniformly-Most-Powerful-Invariant test for detecting a target, know up to a multiplicative factor, in Gaussian noise whose covariance matrix is known but whose power level is unknown. Hence, in order to come up with completely adaptive detection structures against a background of compound-Gaussian clutter, it is necessary to replace in the NMF the covariance matrix with a suitable estimate. The detector obtained is called the Normalized Adaptive Matched Filter (NAMF) [Ran05].

Several estimators have been proposed to estimate the covariance matrix from secondary data collected from cells surrounding the cell under test. Hereafter, we will

briefly review the mostly used in practice. All these estimators are based on the hypothesis that the secondary vectors do not contain interference or targets and share the same covariance matrix as the primary data, the cell under test (CUT) under the null hypothesis.

Before introducing the most popular covariance matrix estimators, it is useful to refer to the problem in its entirety. Thus, the problem of detecting a target signal in additive clutter can be posed in terms of the following binary test:

$$\begin{cases} H_0 : \mathbf{z} = \mathbf{c} & \mathbf{z}_i = \mathbf{c}_i & i = 1,\ldots,K \\ H_1 : \mathbf{z} = \mathbf{s} + \mathbf{c} & \mathbf{z}_i = \mathbf{c}_i & i = 1,\ldots,K \end{cases} \tag{1}$$

where $\mathbf{z}$, $\mathbf{s}$ and $\mathbf{c}$ are the N-dimensional complex vectors of the samples from the baseband equivalents of the received signal, the target and the clutter in the CUT respectively. The set of $\mathbf{z}_1$, $\mathbf{z}_2$,..., $\mathbf{z}_K$ denote the N-dimensional secondary vectors assumed free of signals and interferences. The useful signal $\mathbf{s}$ can be modeled as $\mathbf{s} = \alpha\mathbf{p}$ where $\mathbf{p}$ is the target steering vector and α is an unknown parameter accounting for the channel propagation effect and the target radar cross section. Under the hypothesis of compound-Gaussian clutter each vector $\mathbf{c}_i$ and $\mathbf{c}$ can be modeled as

$$\mathbf{c}_i = \sqrt{\tau_i}\,\mathbf{x}_i, \quad \mathbf{c} = \sqrt{\tau}\mathbf{x},$$

where $\{\mathbf{x}, \mathbf{x}_1, \ldots, \mathbf{x}_K\}$ is a sequence of independent, identically distributed (IID), complex, zero-mean, circular symmetric Gaussian vectors (speckle) with unit power and finite, positive definite covariance matrix, in short notation $\mathbf{x}, \mathbf{x}_i \in C\mathcal{N}(\mathbf{0}, \mathbf{M}_x)$. τ_i and τ (texture) are real, non-negative, random variables independent of $\mathbf{x}_i$ and $\mathbf{x}$.

Finally, for future convenience, we report here the general structure of the NAMF test:

$$\frac{\left|\mathbf{s}^H \hat{\mathbf{M}}^{-1}\mathbf{z}\right|^2}{\left(\mathbf{s}^H \hat{\mathbf{M}}^{-1}\mathbf{s}\right)\left(\mathbf{z}^H \hat{\mathbf{M}}^{-1}\mathbf{z}\right)} \underset{H_1}{\overset{H_0}{\lessgtr}} \lambda \tag{2}$$

where $\hat{\mathbf{M}}$ is any estimate of $\mathbf{M}$ based upon the secondary vectors, namely:

$$\hat{\mathbf{M}} = \hat{\mathbf{M}}(\mathbf{z}_1, \ldots, \mathbf{z}_K) \tag{3}$$

and $\mathbf{M} = \dfrac{1}{\sigma^2} E\{\mathbf{cc}^H\} = \dfrac{\mathbf{M}_c}{\sigma^2}$ is the covariance matrix of the clutter normalized with respect

to its power.

3. Covariance matrix estimators

In this paragraph we describe three of the most popular estimators of the clutter covariance matrix.

a) Sample covariance matrix: **SCM**.

It is an estimator of $\mathbf{M}_c$ and it is given by:

$$\hat{\mathbf{M}}_{SCM} = \frac{1}{K} \sum_{i=1}^{K} \mathbf{z}_i \mathbf{z}_i^H = \frac{1}{K} \sum_{i=1}^{K} \tau_i \left(\mathbf{x}_i \mathbf{x}_i^H \right). \tag{4}$$

Plugging the $\hat{\mathbf{M}}_{SCM}$ into (2) we obtain a detector that is CFAR only with respect to $\mathbf{M}_c$ and whose probability of false alarm (P_{FA}) strongly depends on the distribution of the texture [Gin02], [Con02a], [Con02c]. The estimator (4) is ML when the clutter is Gaussian distributed, then when the texture values τ_i are all equal and deterministic. It is also the ML estimator when the τ_i are random but completely correlated, i.e. $\tau = \tau_1 = \dots = \tau_K$ [Ric96]. The performance of this matrix estimator in presence of compound-Gaussian clutter has been investigated in [Gin99].

b) Normalized sample covariance matrix: **NSCM**.

It is an estimator of $\mathbf{M}$ and it is given by:

$$\hat{\mathbf{M}}_{NSCM} = \frac{N}{K} \sum_{i=1}^{K} \frac{\mathbf{z}_i \mathbf{z}_i^H}{\mathbf{z}_i^H \mathbf{z}_i} = \frac{N}{K} \sum_{i=1}^{K} \frac{\mathbf{x}_i \mathbf{x}_i^H}{\mathbf{x}_i^H \mathbf{x}_i} \tag{5}$$

It is very similar to the SCM estimate but it uses normalized secondary data, then its distribution does not depend on the texture pdf but only on the speckle distribution. Plugging the $\hat{\mathbf{M}}_{NSCM}$ into (2) we obtain a detector that is CFAR with respect to the statistics of the texture and to the clutter power. Unfortunately the normalization with respect to $\mathbf{z}_i^H \mathbf{z}_i / N$ makes the NAMF detector no longer CFAR with respect to $\mathbf{M}$ [Gin02],

[Con02a], [Con02c]. The performance of the NSCM matrix estimator in presence of compound-Gaussian clutter has been investigated in [Gin99] and [Bau07].

c) Fixed point and maximum likelihood estimator

The fixed point estimator (FPE) arises as an approximation of the ML estimation [Gin02] (it has been termed FPE in [Pas07]). It is defined as a fixed point of the function:

$$f_{K,\mathbf{M}} : \begin{cases} \mathcal{D} \to & \mathcal{D} \\ \mathbf{A} \to & \dfrac{N}{K} \sum_{i=1}^{K} \dfrac{\mathbf{z}_i \mathbf{z}_i^H}{\mathbf{z}_i^H \mathbf{A}^{-1} \mathbf{z}_i} \end{cases} \tag{6}$$

where $\mathcal{D} = \left\{ \mathbf{A} \in M_N(\mathbb{C}) \middle| \mathbf{A}^H = \mathbf{A}, \mathbf{A} \text{ positive definite} \right\}$ with $M_N(\mathbb{C}) = \{ N \times N$ matrices with elements in $\mathbb{C} \}$. As shown in [Pas07], equation $\hat{\mathbf{M}} = f_{K,\mathbf{M}} \left(\hat{\mathbf{M}} \right)$ has a solution of the form $\alpha \mathbf{M}$, where α is an arbitrary scaling factor. The only solution $\hat{\mathbf{M}}$ satisfying the normalization $Tr \left(\mathbf{M}^{-1} \hat{\mathbf{M}} \right) = N$ is called the Fixed Point (FP) estimate, $\hat{\mathbf{M}}_{FP}$.

In other words, $\hat{\mathbf{M}}_{FP}$ is the unique solution of

$$\hat{\mathbf{M}}_{FP} = \frac{N}{K} \sum_{i=1}^{K} \frac{\mathbf{z}_i \mathbf{z}_i^H}{\mathbf{z}_i^H \hat{\mathbf{M}}_{FP}^{-1} \mathbf{z}_i} = \frac{N}{K} \sum_{i=1}^{K} \frac{\mathbf{x}_i \mathbf{x}_i^H}{\mathbf{x}_i^H \hat{\mathbf{M}}_{FP}^{-1} \mathbf{x}_i} \tag{7}$$

satisfying $Tr \left(\mathbf{M}^{-1} \hat{\mathbf{M}}_{FP} \right) = N$. Notice that $\hat{\mathbf{M}}_{FP}$ does not depend on the texture values τ_i. This property is of great importance in practice. As verified in [Pas07], the FP is the ML estimate when the texture is assumed to be an unknown deterministic parameter and an Approximate Maximum Likelihood (AML) estimate when the texture is assumed to be a non negative random variable [Gin02].

To find the FP solution, we must resolve the transcendental equation (7). In [Gin02] the authors developed an iterative algorithm to calculate this solution in the case of random texture. The iterative algorithm is given by the following equation

$$\hat{\mathbf{M}}(k+1) = \frac{N}{K} \sum_{i=1}^{K} \frac{\mathbf{z}_i \mathbf{z}_i^H}{\mathbf{z}_i^H \hat{\mathbf{M}}(k)^{-1} \mathbf{z}_i} \tag{8}$$

where k is the kth iteration. A deep analysis of this algorithm and its convergence rate as a function of the number of secondary vectors K, the number of pulses N, and the shape of the clutter covariance function can be found in [Gin02] and [Pas07]. Generally the number of iterations N_{it} necessary to guarantee the convergence is small (say 2 or 3). In [Gin02] it was also verified by simulation that the NAMF that uses the AML matrix estimator is almost insensitive to the shape of the covariance matrix, then it can be considered CFAR with respect to the texture distribution and very robust with respect to the covariance matrix. In [Con02c] the authors proved that if the clutter spectrum is symmetric about the frequency f=0 and the initialization matrix of the iterative procedure (8) is done by

$$\mathbf{\Sigma}^{(0)} = \frac{1}{K} \sum_{i=1}^{K} \frac{\mathbf{z}_i^{(1)} \mathbf{z}_i^{(1)T}}{\left(\mathbf{z}_i^{(2)} \mathbf{z}_i^{(2)T}\right)_{kk}} \tag{9}$$

where $\mathbf{z}_i^{(1)}$ and $\mathbf{z}_i^{(2)}$ are the real and imaginary part of the complex vector $\mathbf{z}_i$ respectively, and $\mathbf{A}_{kk}$ is the (i,i)th element of the $N \times N$ matrix $\mathbf{A}$, then the NAMF is CFAR also with respect to $\mathbf{M}$. This is not true if the spectrum is not symmetrically shaped around f=0, as it is always in sea clutter scenarios.

4. Statistical data analysis

The goal of this technical report is to investigate the CFAR property of the NAMF detector of eq. (2) with respect to the covariance structure and the texture statistics using each of the three matrix estimators reviewed in the previous paragraph in real sea clutter data, recorded by the IPIX radar. Table 1 shows the specifications of the analyzed files 19980223_165836_antstep, 19980227_213016_antstep and 19980227_213808_antstep.

The number of range cells for the file 19980223_165836_antstep is 34, but unfortunately, the last 5 (30-34) contain a target (maybe a small object floating on the waves), then only 29 cells can be considered in our analysis. In the other files there is not target and the range cells are 28.
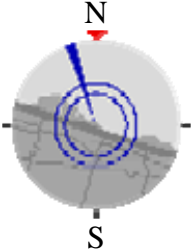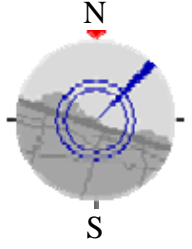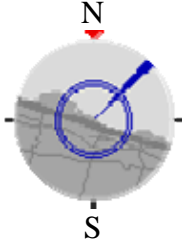
Name of the data set	19980223_165836_antstep	19980227_213016_antstep	19980227_213808_antstep
Date, time of acquisition	23/02/1998 16:58:36	27/02/1998 21:30:16	27/02/1998 21:38:08
#Range cells	34	28	28
Start range	3201 m??		
Range resolution	30 m	30 m	15 m
Pulse width	200 ns	200 ns	100 ns
Total # sweep	60000	60000	60000
Sample for cell	60000 Sampled at 30 m	60000 Sampled at 30 m	60000 Sampled at 15 m
PRF	1 KHz	1 KHz	1 KHz
Frequency RF	9.39 GHz	9.39 GHz	9.39 GHz
Radar and wave geometry			

Table 1 - Characteristics of the analyzed files.

The data have been previously processed in order to remove the dc offset and the phase imbalance due to hardware imperfections and then stored in an $N_t \times N_c$ complex matrix. A detailed statistical analysis of adopted real data has been performed as in [Gre06] and in [Gin06]. The results have shown a reasonable fit of the data to the K model.

The shape parameter ν is not constant on all the range cells. In Figs.1-3 we show the estimated values for VV and HH data for the three files. As expected the values of ν for the HH data are always lower than that for the VV data, then the HH polarization is spikier than the VV. The ratio between the ν parameters of the VV data and the HH data is close to 0.9 for each cell and each analyzed file. The mean value of ν for the VV data and HH data are reported in table 2. The spikiest data are those of file 19980227_213016_antstep.

File name	VV	HH
19980223_165836_antstep	0.7563	0.4355
19980227_213016_antstep	0.6434	0.3981
19980227_213808_antstep	1.0046	0.5141

Table 2 - ν_{mean} for the analyzed files.
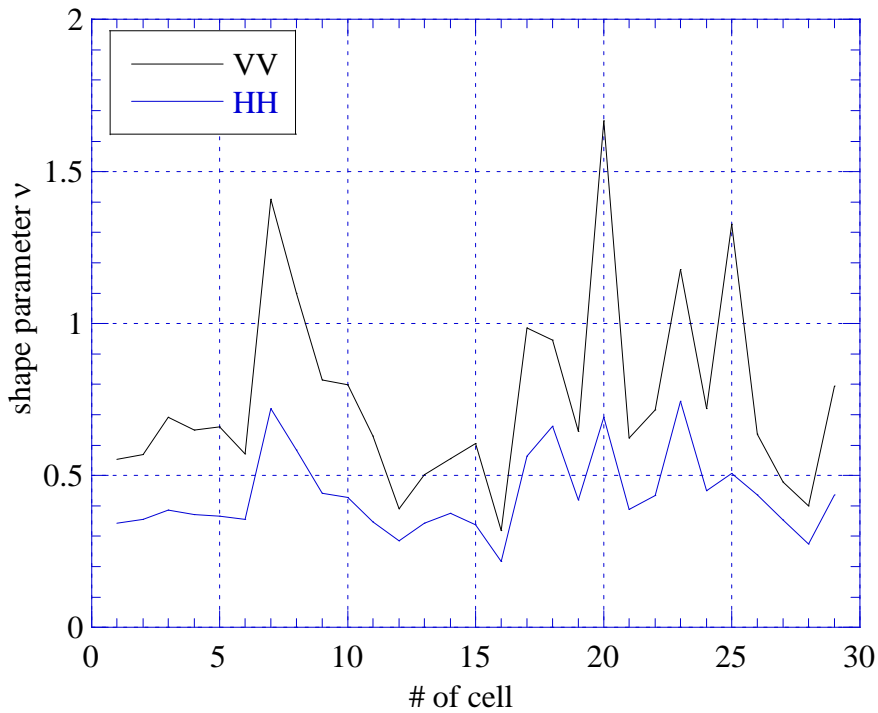
Fig. 1 – File 19980223_165836_antstep.
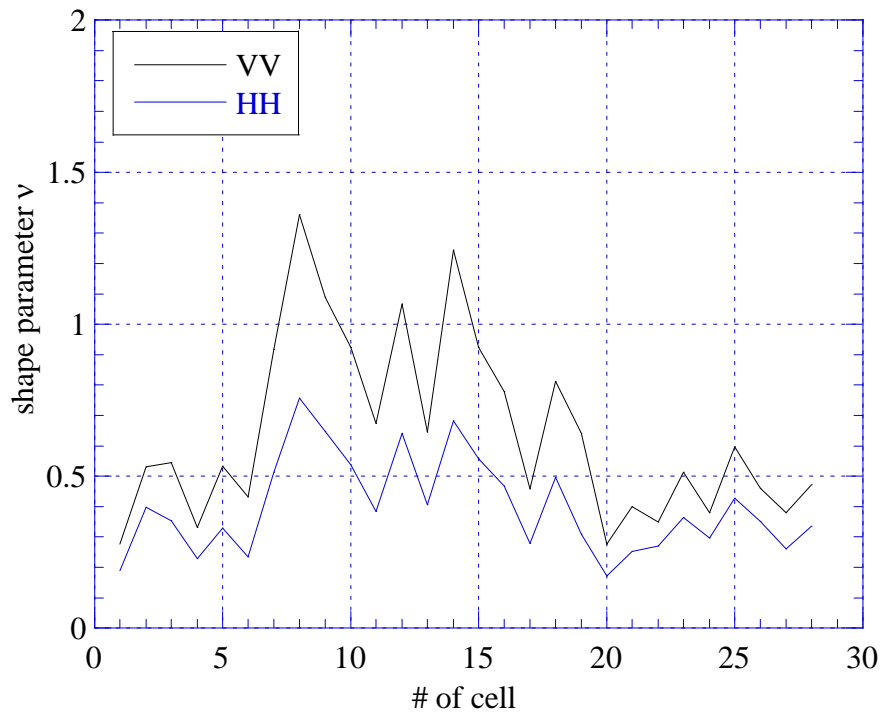
Fig. 2 – File 19980227_213016_antstep.
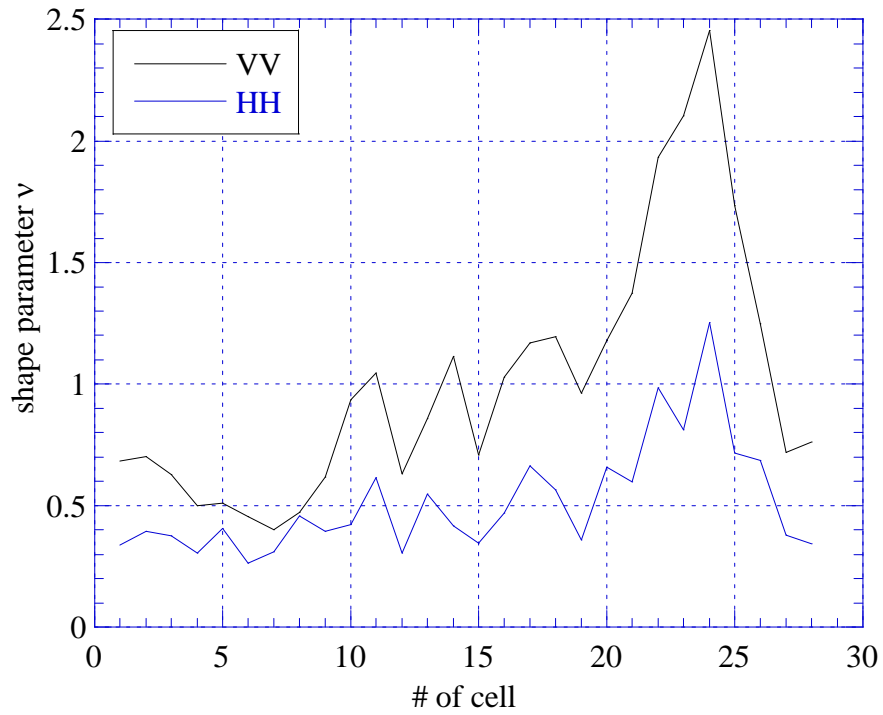
Fig. 3 – File 19980227_213808_antstep.

11

5. Spectral analysis

We estimated also the powers spectral density (PSD) of the clutter in each range cell by means of Welch modified periodogram with rectangular windows of 256 samples and an overlap of 50 %. The results are reported in Figs. 4 and 5 for the 1st file (19980223_165836_antstep), where the periodogram normalized with respect to the estimated power for the 29 cells is plotted in a color scale from blue to red, as a function of the number of cell and the normalized (with respect to the radar PRF) frequency. The spatial non stationarity of the clutter is evident, the PSD varies from cell to cell. The peak of the PSD is generally between $f=0.05$ and $f=0.1$, as verified also in Fig. 6 where the average PSD is reported for both polarizations. The average PSD has been calculated as the mean of the periodograms estimated on the 29 cells.

We obtain similar results for the 2nd and the 3rd files as shown in Figs. 7-9 for file 19980227_213016_antstep and Figs.10-12 for file 19980227_213808_antstep.
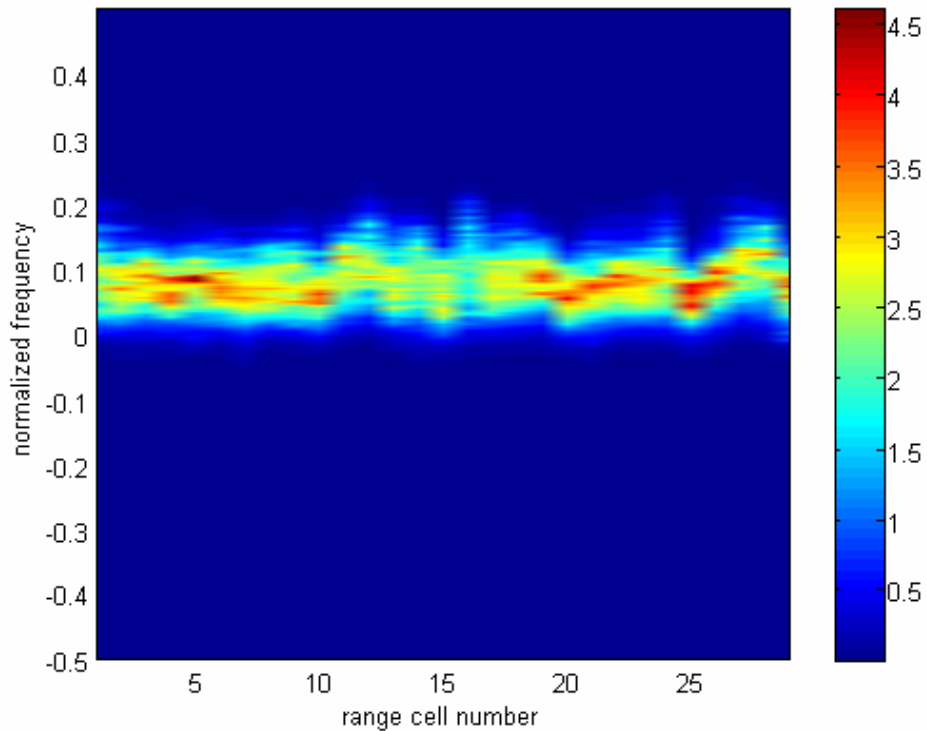
Fig. 4 – PSD of sea clutter as a function of range cell number, VV data, 1st file.
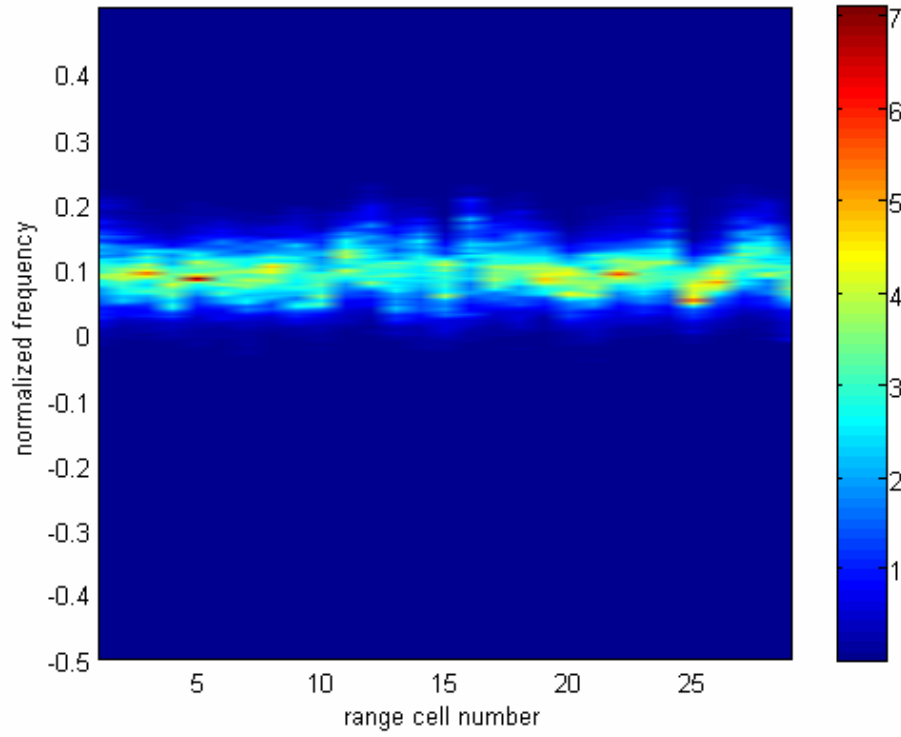
Fig. 5 – PSD of sea clutter as a function of range cell number, HH data, 1st file.
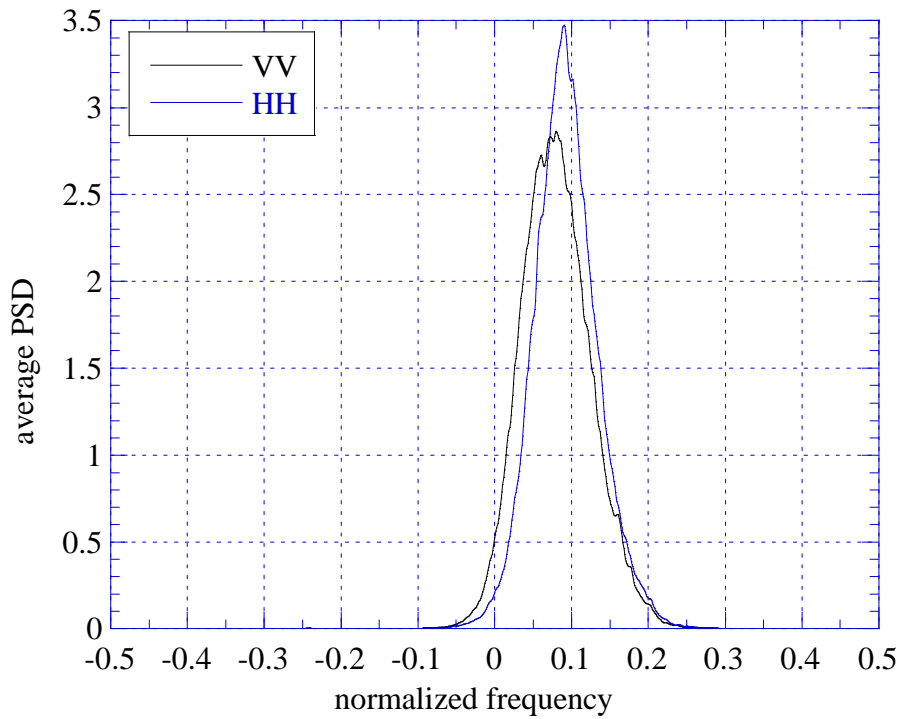
Fig. 6 – Average PSD of sea clutter, 1st file.

13
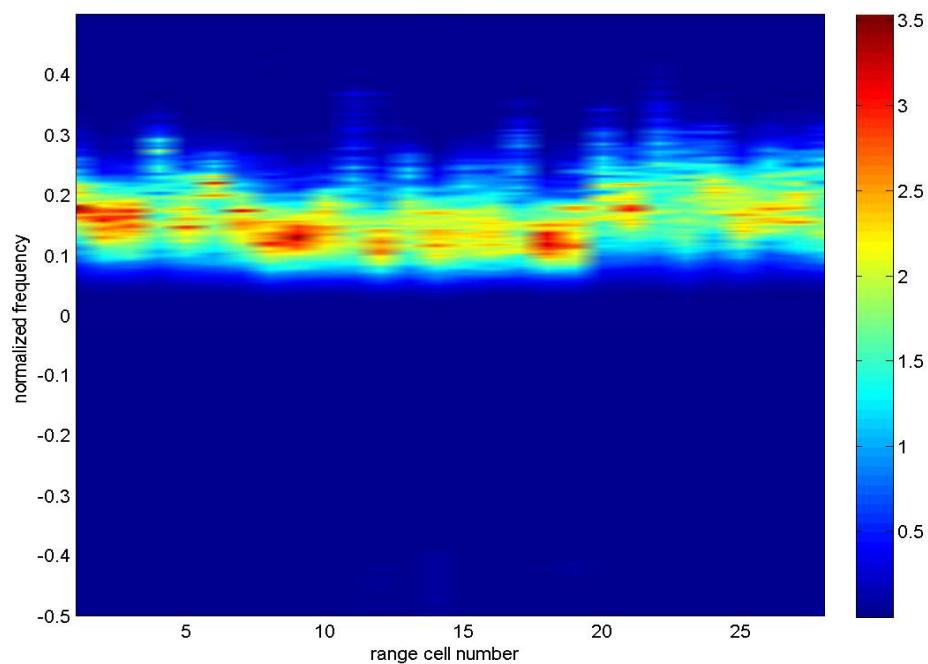
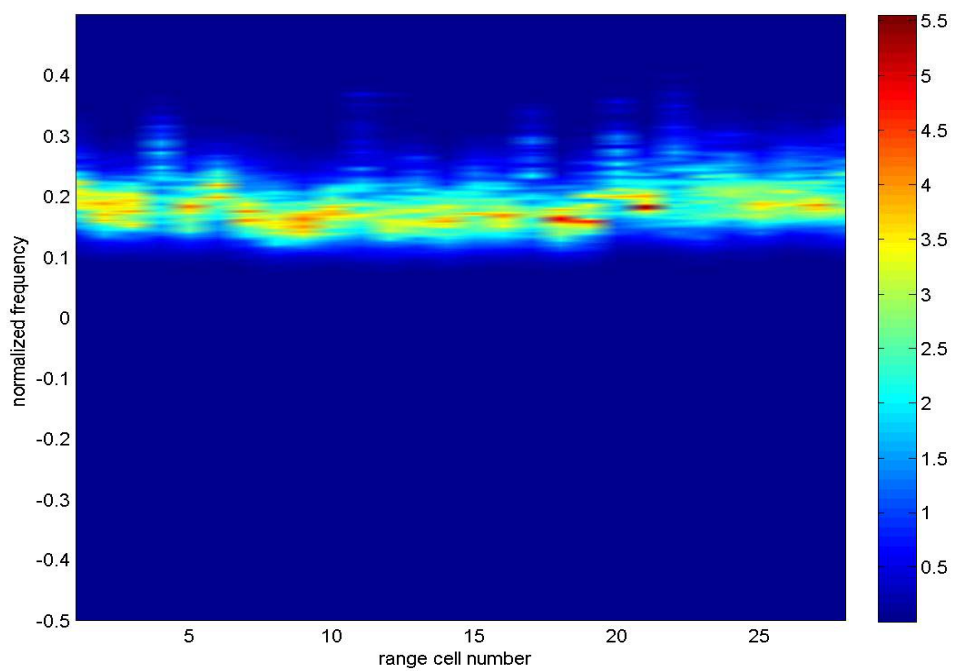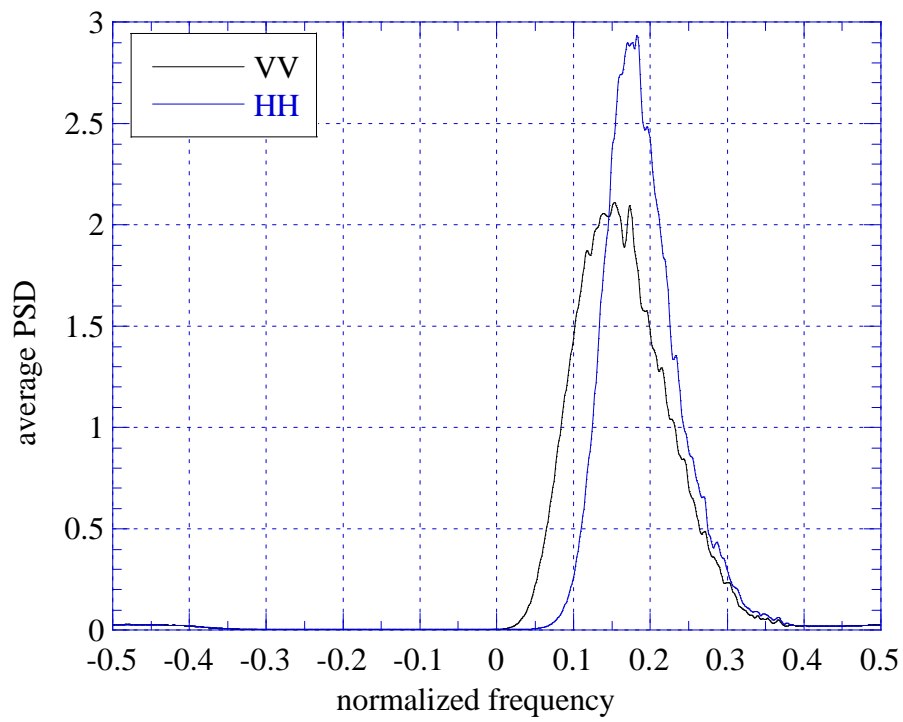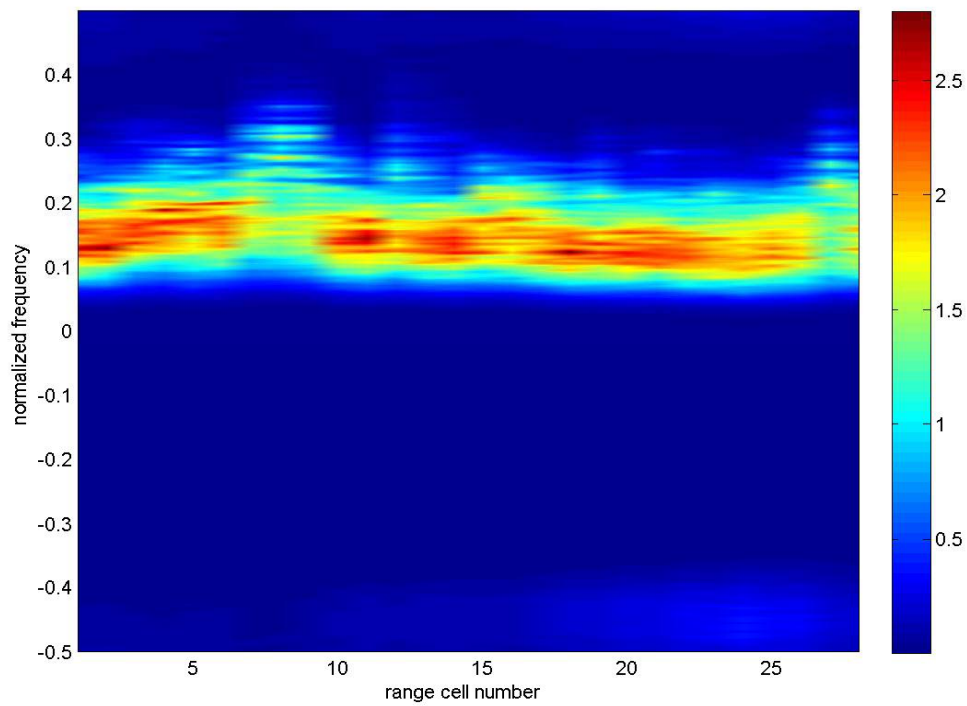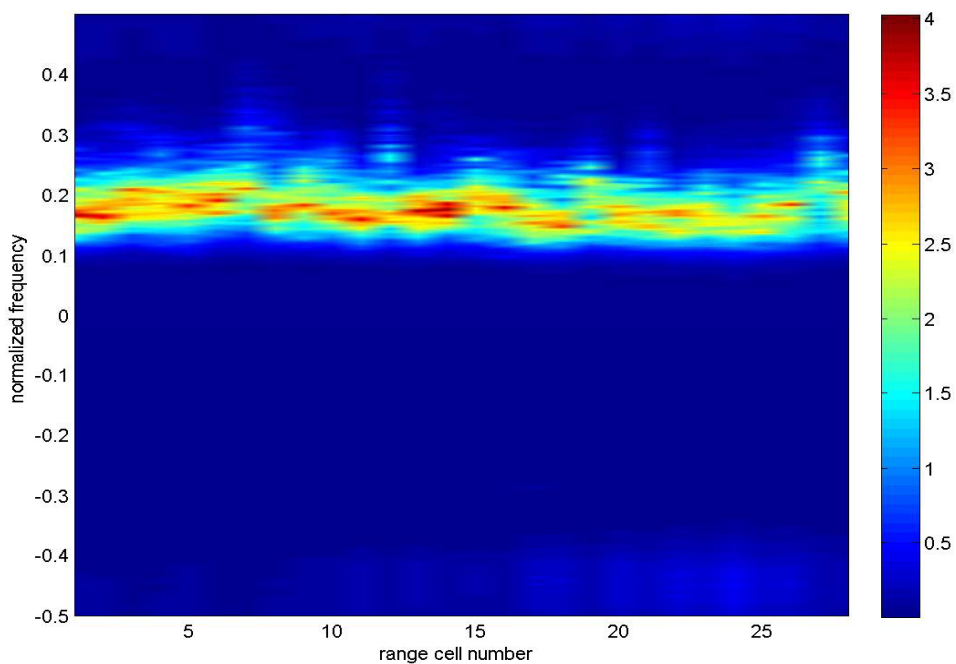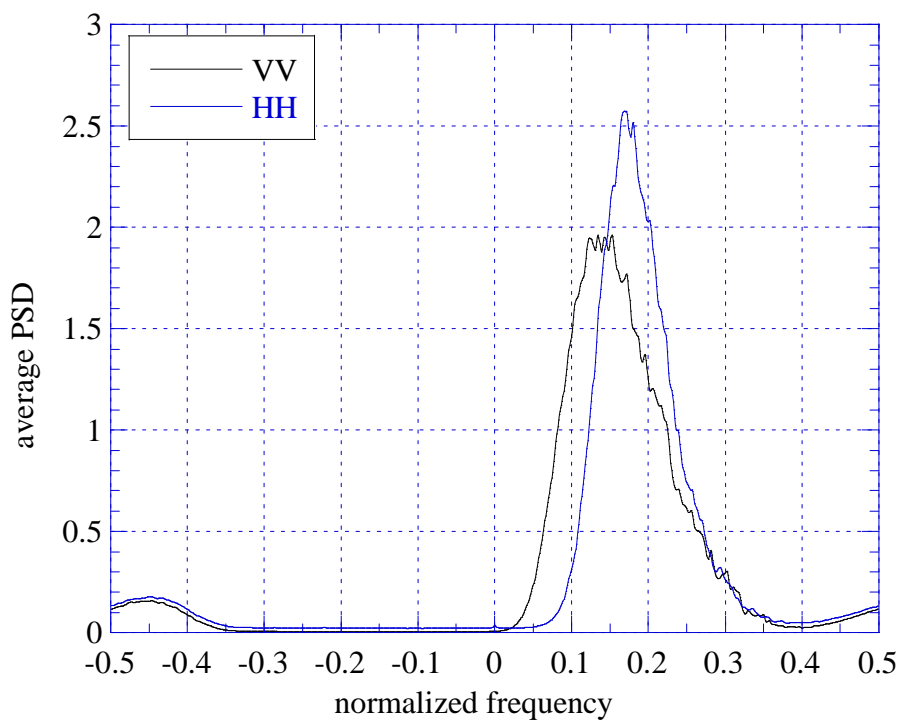**Fig. 7** – PSD of sea clutter as a function of range cell number, VV data, 2nd file.

Fig. 8 – PSD of sea clutter as a function of range cell number, HH data, 2nd file.

Fig. 9 – Average PSD of sea clutter, 2nd file.

Fig. 10 – PSD of sea clutter as a function of range cell number, VV data, 3rd file.

Fig. 11 – PSD of sea clutter as a function of range cell number, HH data, 3rd file.

Fig. 12 – Average PSD of sea clutter, 3rd file.

To complete the spectral analysis, we calculated also the spectrogram of the data for each range cell as in [Gin06]. For the 1st file we show here only the results for the 11th cell, in Figs. 13 and 14 for VV and HH data respectively. In both the polarizations the behavior is similar and some temporal periodicities are apparent, particularly in the ranges 5-20 sec and 35-50 sec. Again the temporal non-stationary behavior of the sea clutter is evident.

For the 2nd file we report in this section the results for the 1st, 4th and 11th range cell in Figs. 15-20. For the 3rd file we report the 7th, 13th and 27th in Figs. 21-25 for both polarizations. Also in these two files the temporal non-stationarity is apparent.
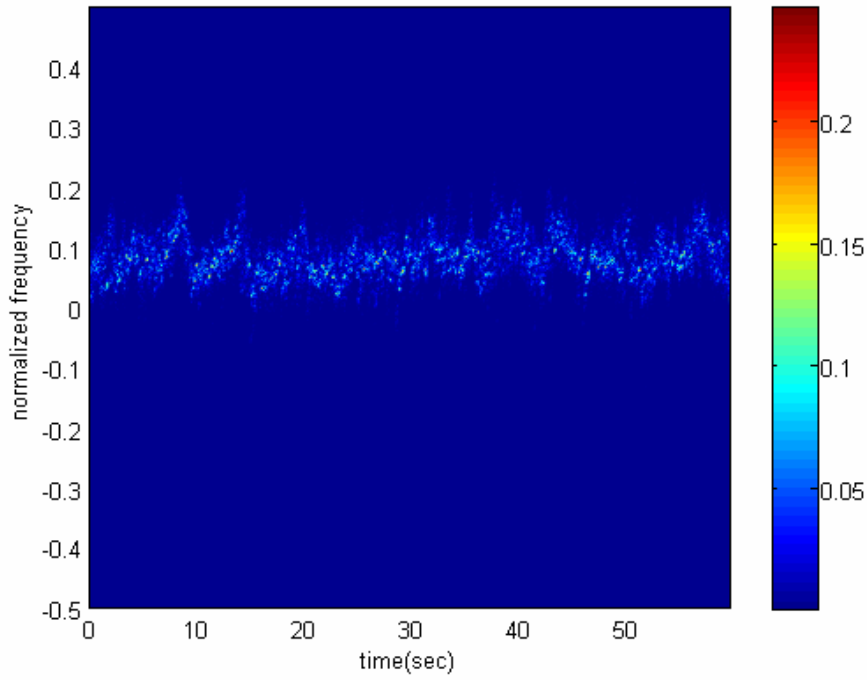
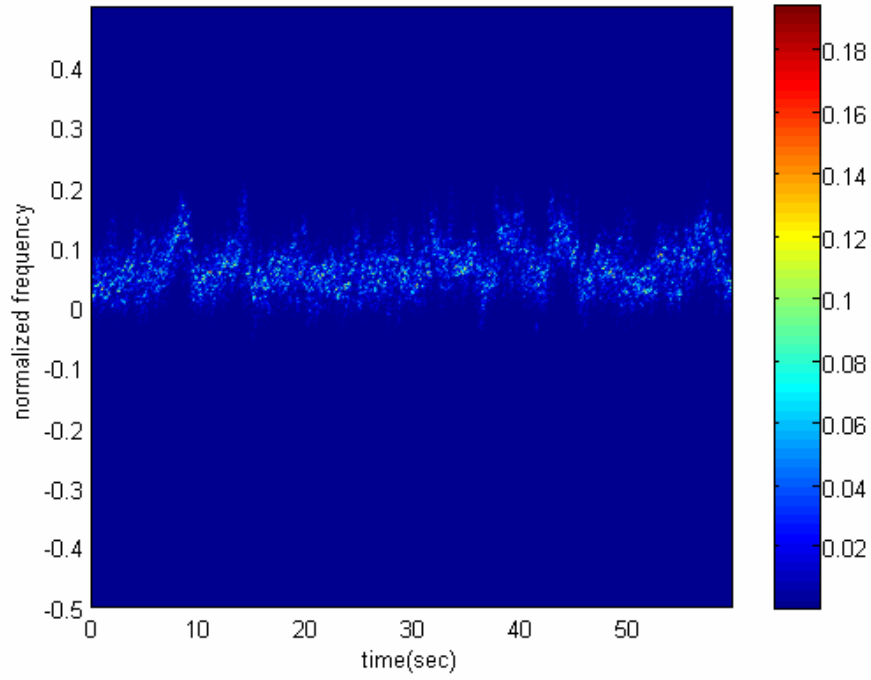**Fig. 13** – Spectrogram of sea clutter, 11th cell, VV data, 1st file.

17

Fig. 14 – Spectrogram of sea clutter, 11th cell, HH data, 1st file.
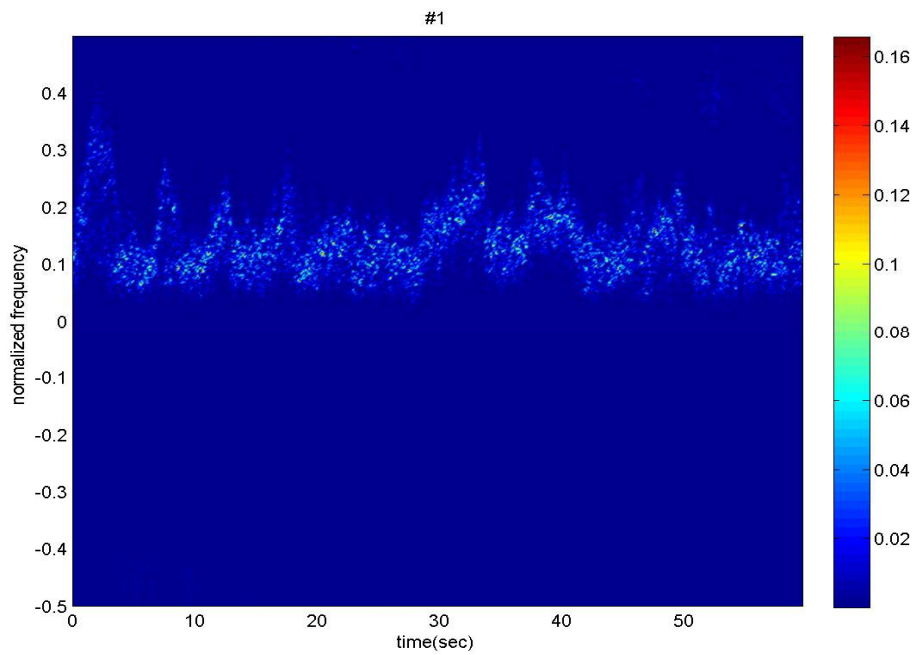

Fig. 15 – Spectrogram of the 1st cell, VV data, 2nd file.
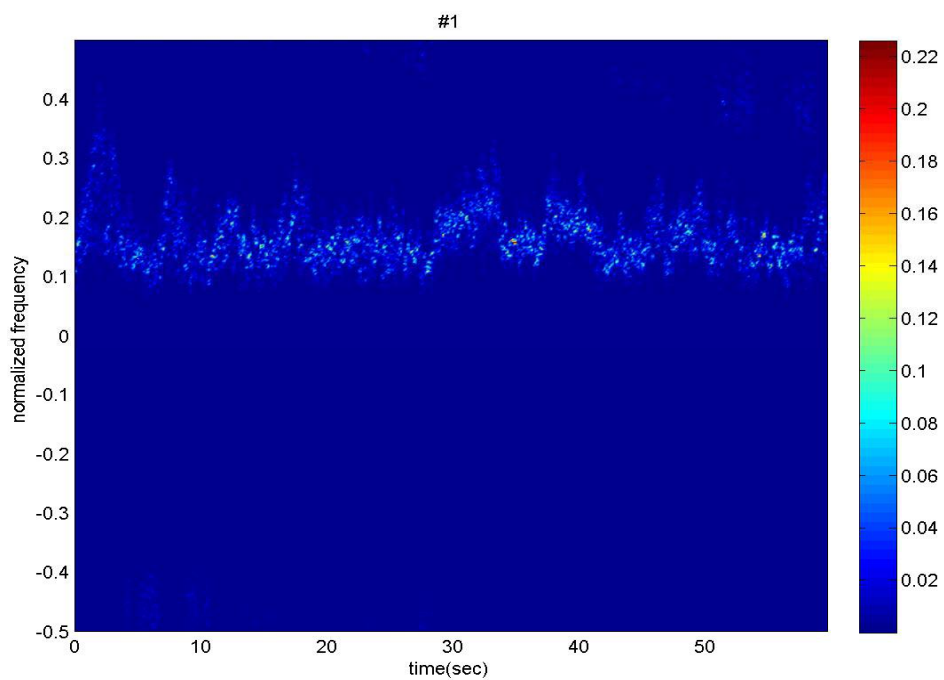
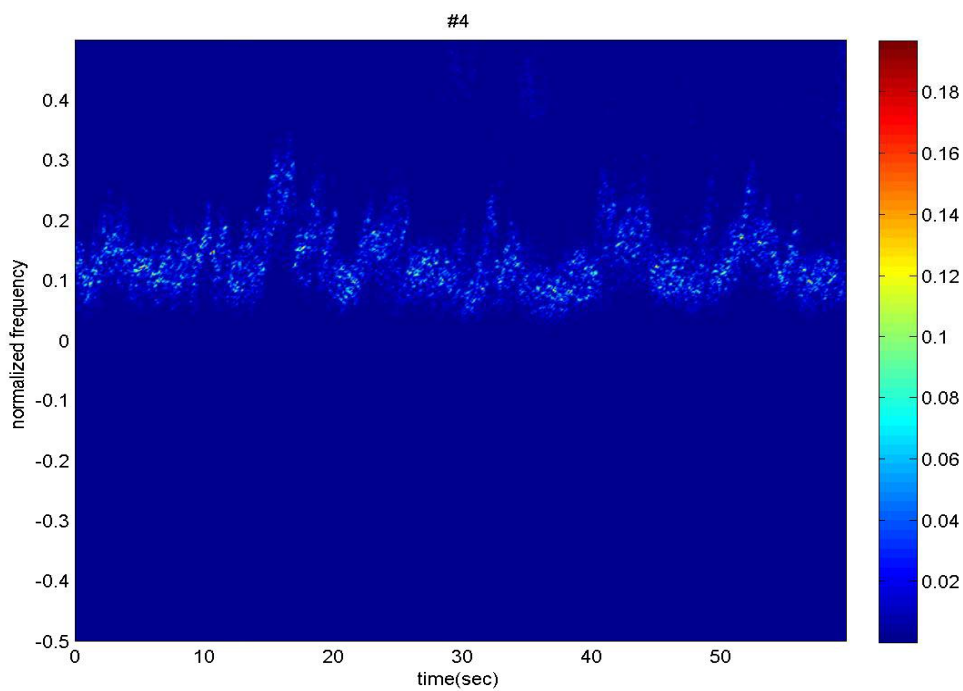**Fig. 16** – Spectrogram of the 1st cell, HH data, 2nd file.

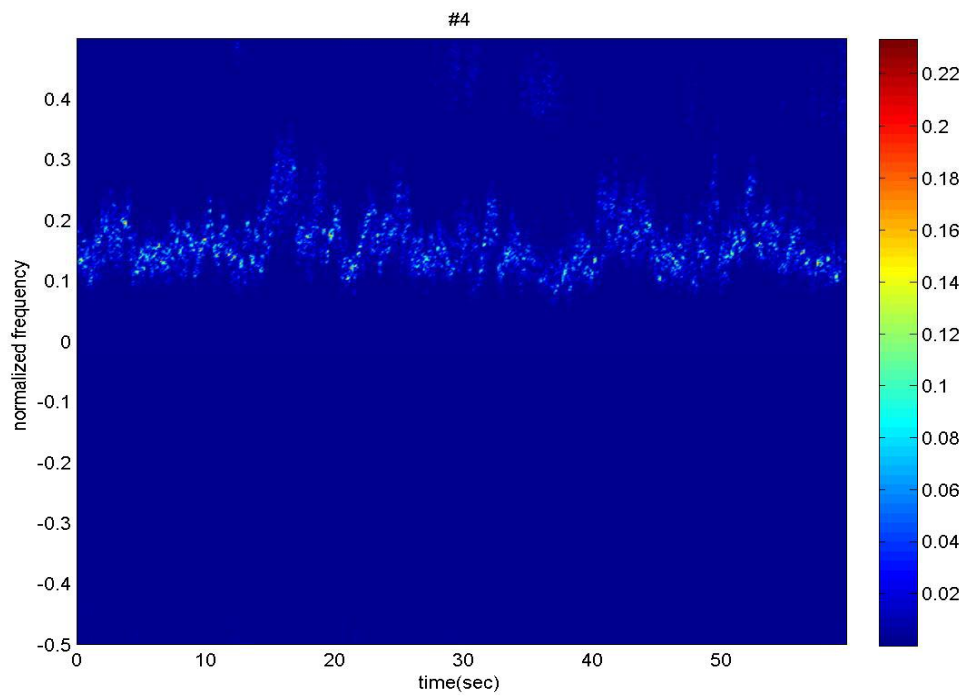**Fig. 17** – Spectrogram of the 4th cell, VV data, 2nd file.

19

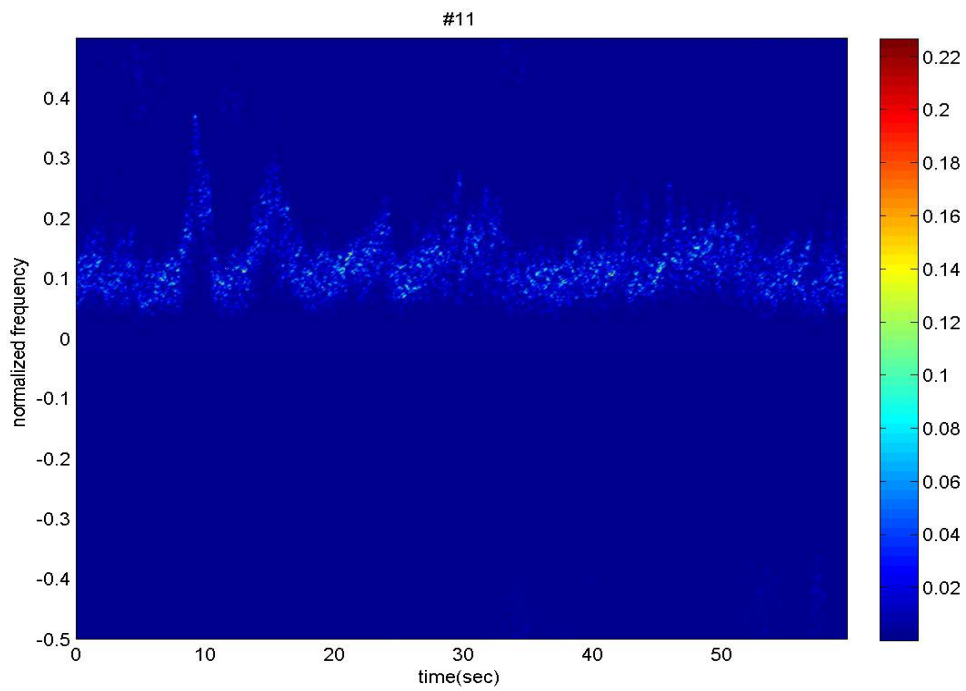**Fig. 18** – Spectrogram of the 4th cell, HH data, 2nd file.

Fig. 19 – Spectrogram of the 11th cell, VV data, 2nd file.

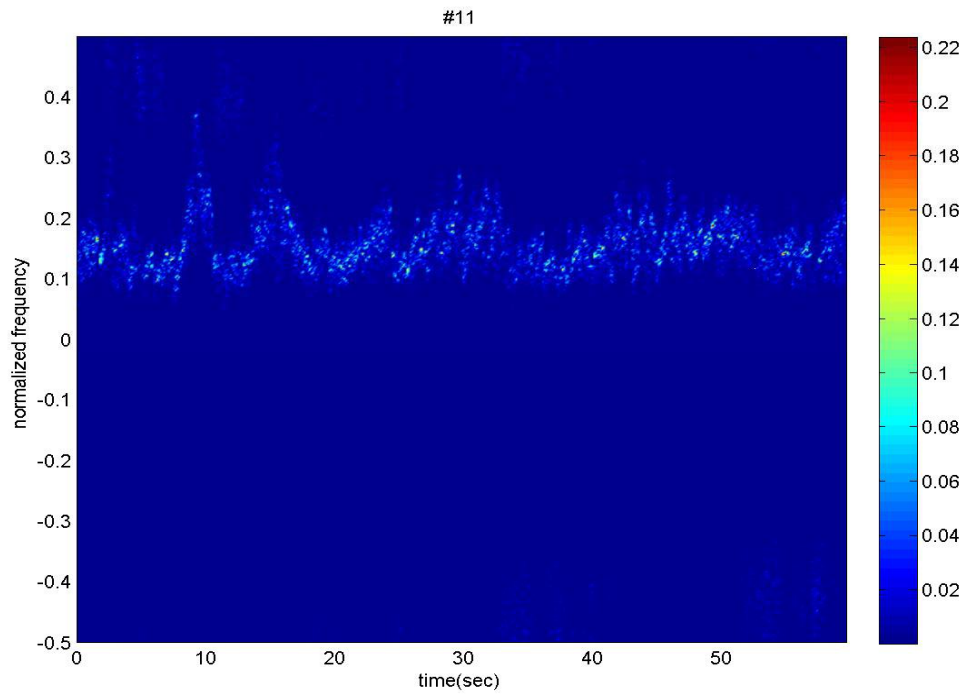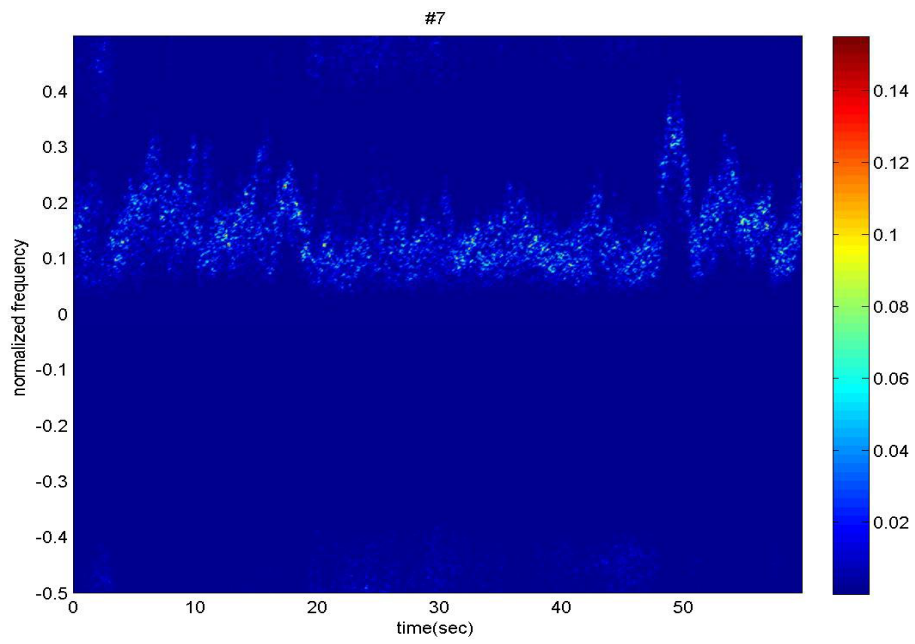**Fig. 20** – Spectrogram of the 11th cell, HH data, 2nd file.

Fig. 21 – Spectrogram of the 7th cell, VV data, 3rd file.
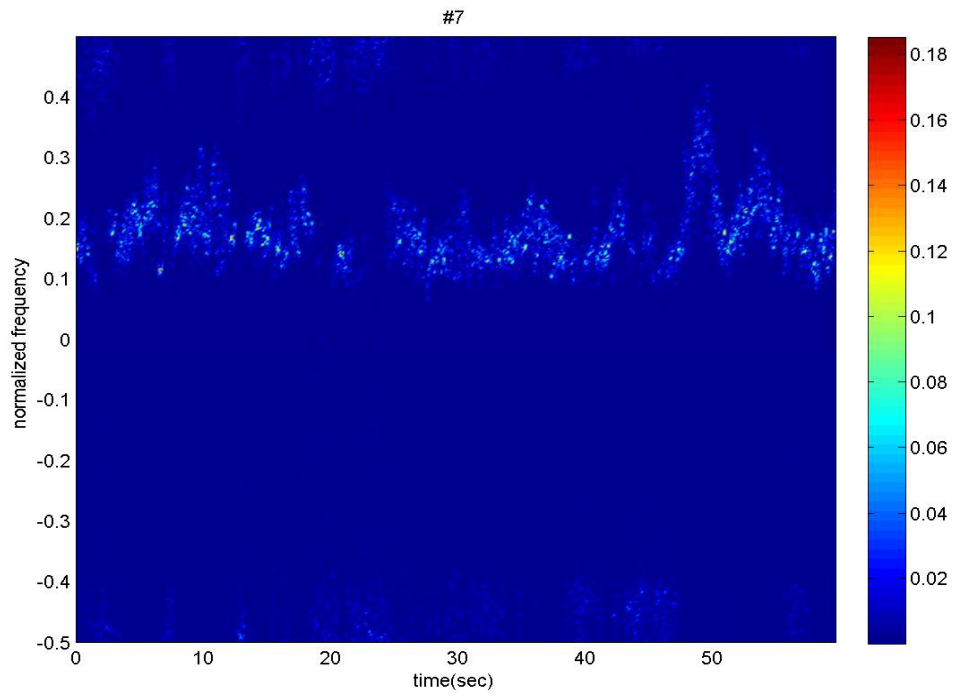
21

Fig. 22 – Spectrogram of the 7th cell, HH data, 3rd file.
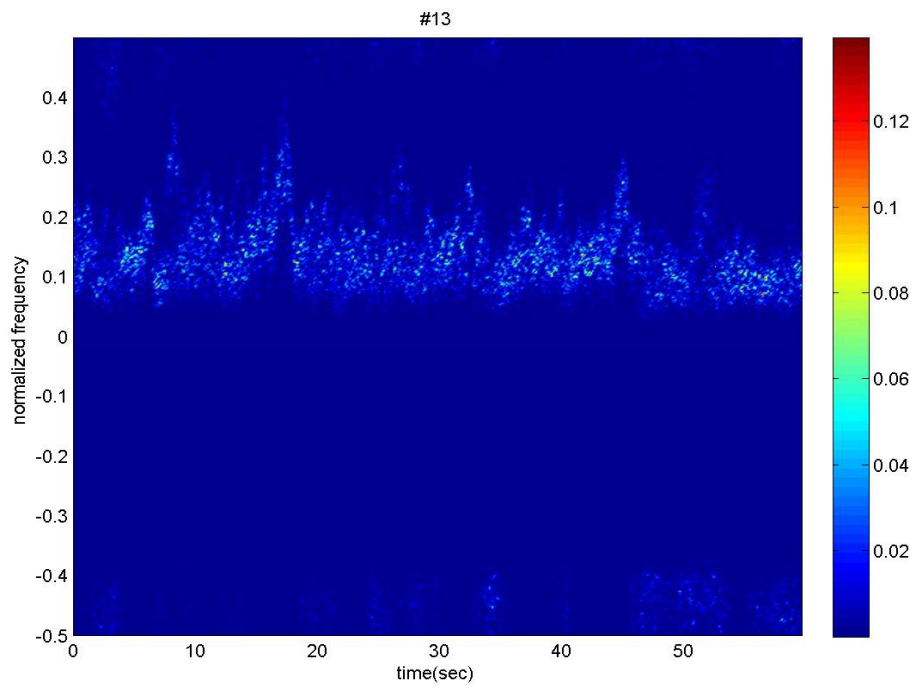

Fig. 23 – Spectrogram of the 13th cell, VV data, 3rd file.
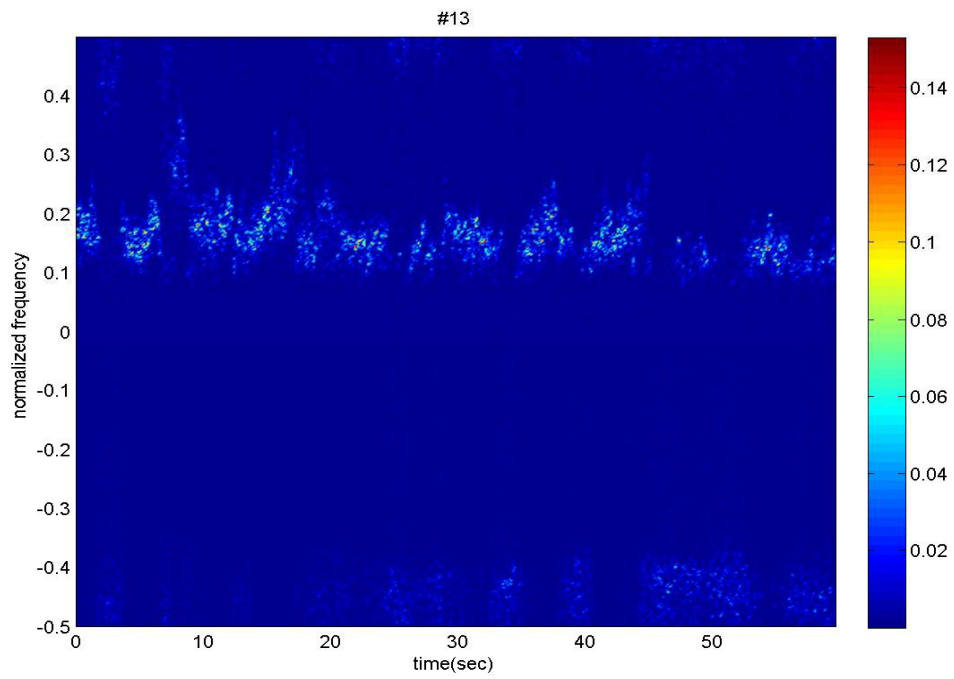
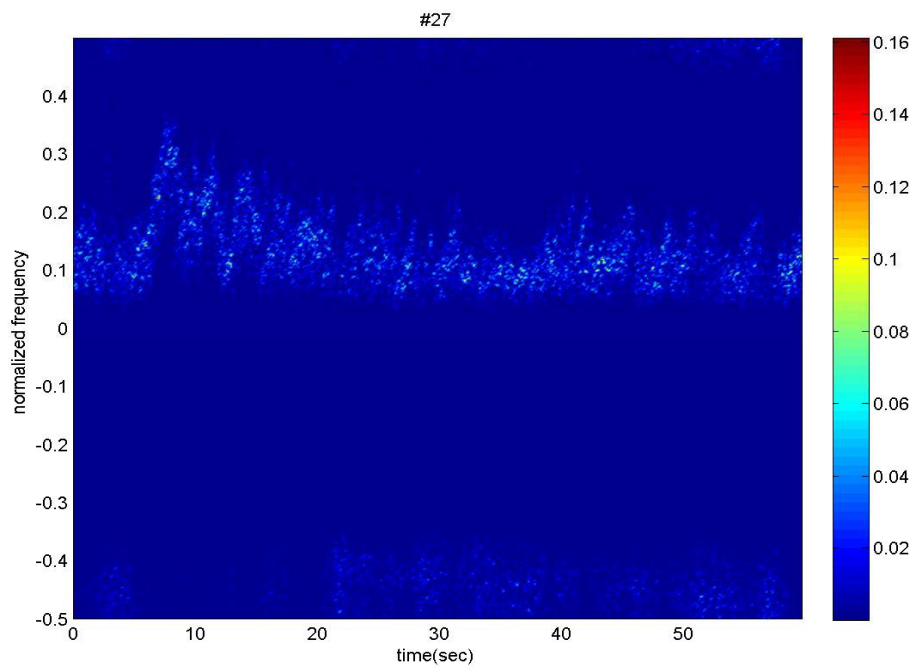**Fig. 24** – Spectrogram of the 13th cell, HH data, 3rd file.

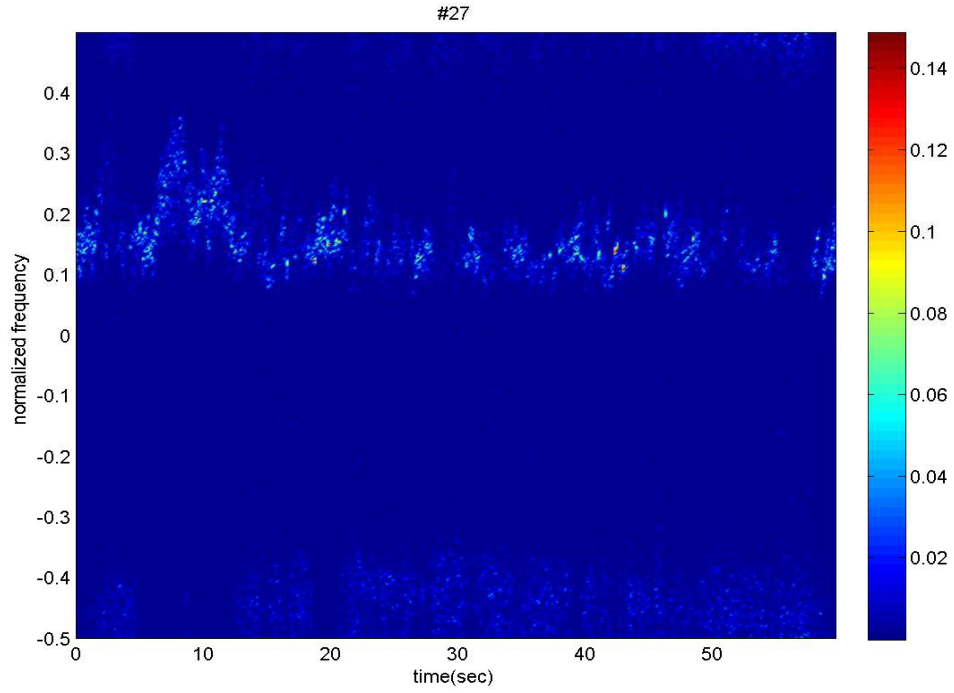**Fig. 25** – Spectrogram of the 27th cell, VV data, 3rd file.

Fig. 26 – Spectrogram of the 27th cell, HH data, 3rd file.

Summarizing our results on the statistical analysis on sea clutter file we can state that:

1. The sea clutter show a good fit to K model but the shape parameter of the distribution changes from cell to cell.
2. The speckle PSD is not constant in time and space, so the clutter is not spatially and temporally stationary. The spectrogram evidences some temporal periodicity in spectrum PSD behavior.

The aim of the analysis described in the following sections is to verify and measure the impact of these spatially and temporally non-stationarity on the CFARness and in general on the performance of the NAMF.

24

6. Performance analysis and CFAR property

The procedure used to assess the performances is now described. We consider an $N \times (K+1)$ data window, where N is the number of pulses and K the number of secondary cells, the primary cell (CUT) is set in the middle of the window. The data window is slid in space from range bin to range bin and in time with an overlap of 50 % ($N/2$ samples) until the end of the dataset. The overall number of trials is:

$$N_{trials} = \frac{(N_s - N/2)}{N/2}(N_c - K - 1),$$

where N_s=60000 and N_c=29. Moreover, for evaluating the performance of the NAMF, we set N=8 and K=16. The steering vector of the signal is:

$$\mathbf{p} = \left[1, \exp(j2\pi f_D), \ldots, \exp(j2\pi(N-1)f_D)\right]^T,$$

where f_D is the normalized Doppler frequency of the target.

In analyzing the behavior of the NAMF with the real data our aim is to highlight the impact of clutter non-stationarity on the false alarm rate (FAR). As written in Section 3, we know that:

(*i*) the NAMF with the SCM is CFAR with respect to $\mathbf{M_c}$ and to $\mathbf{M}$, but not with respect to the statistics of the texture;

(*ii*) the NAMF with the NSCM is CFAR with respect to the statistics of the texture, but not with respect to $\mathbf{M}$;

(*iii*) the NAMF with the FP is CFAR with respect to the statistics of the texture, and very robust with respect to $\mathbf{M}$.

Then, to set the threshold for a nominal probability of false alarm $P_{FA0} = 10^{-1}$ and $P_{FA0} = 10^{-2}$ in the NAMF with each of the three matrix estimators, we generated K-distributed clutter with covariance matrix equal to the average covariance matrix of the real data and with shape parameter equal to the estimated ν_{mean}. The average covariance matrix has been built based on the estimated correlation as:

$$\hat{R}(m) = \frac{1}{N_c N} \sum_{k=1}^{N_c} \sum_{i=0}^{N-|m|-1} z_k(n) z_k^*(n+m) \qquad (10)$$

where $z_k(n)$ in the nth sample of the kth range cell on the clutter complex envelope.[1] Running Monte Carlo simulation with this simulated data for different values of the target Doppler frequency f_D, we observed that, even if the NAMF-NSCM and the NAMF-FP are not CFAR with respect to **M**, the nominal threshold shows very small variations as function of f_D and it can be practically considered constant. The nominal thresholds are reported in Table 3 for the 1$^{\text{st}}$ file.

	$P_{FA}=10^{-1}$	$P_{FA}=10^{-2}$
SCM	0.537	0.760
NSCM	0.460	0.682
FP	0.485	0.712

Table 3a – NAMF threshold values, N=8, K=16, VV data

	$P_{FA}=10^{-1}$	$P_{FA}=10^{-2}$
SCM	0.604	0.816
NSCM	0.456	0.680
FP	0.484	0.710

Table 3b – NAMF threshold values, N=8, K=16, HH data

After setting the nominal thresholds we estimated by Monte Carlo simulation the probability of false alarm of the NAMF fed by the real data in both the polarizations. The results are shown for the 1$^{\text{st}}$ file in Figs. 27-28 for the VV data and Figs. 29-30 for the HH data as a function of the target Doppler frequency f_D.

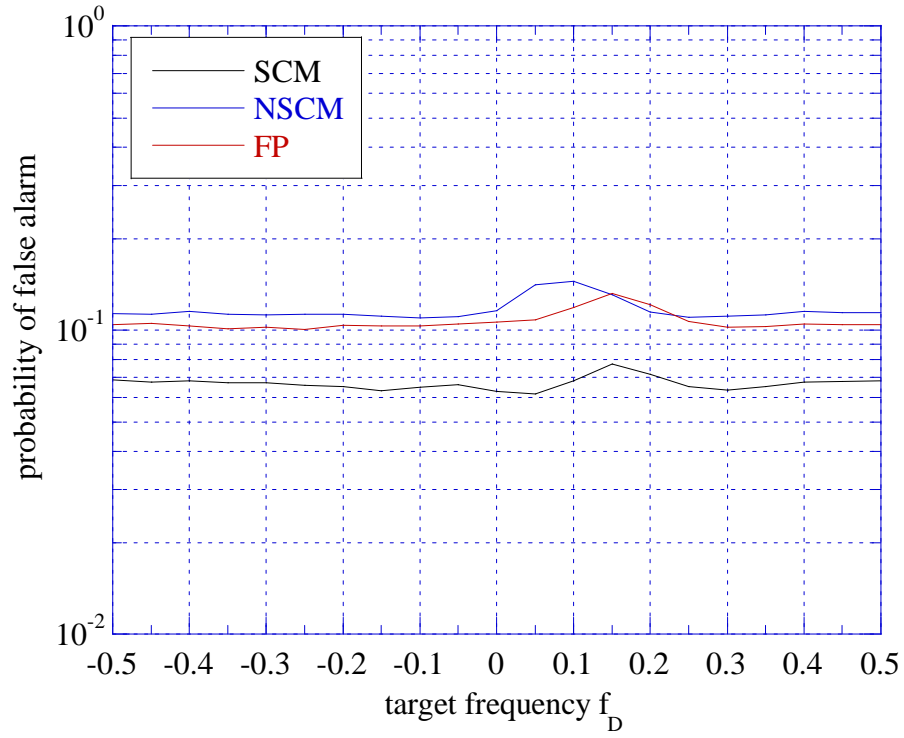[1] The mean value for each range cell has been subtracted before processing the data.

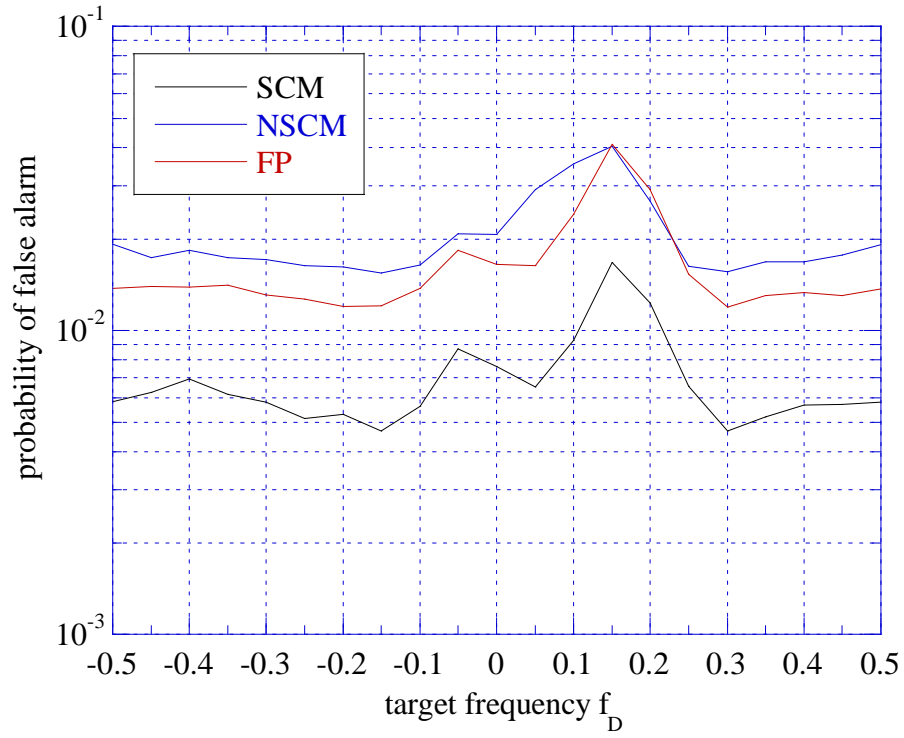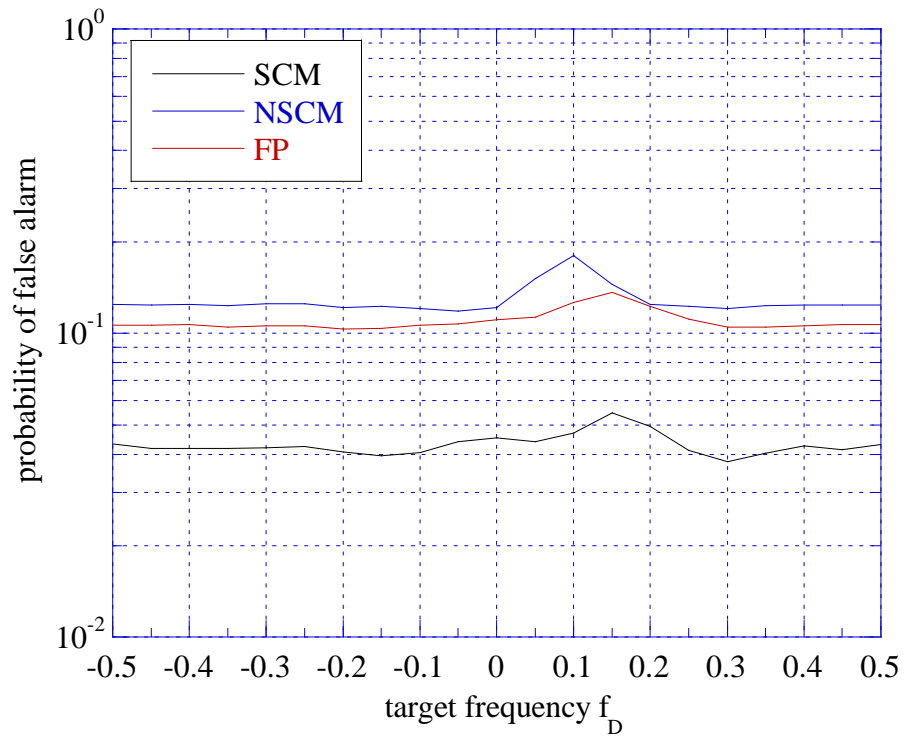**Fig. 27** – Probability of false alarm with real VV data, N=8, K=16, P_{FA0}=10^{-1}, 1st file.

Fig. 28 – Probability of false alarm with real VV data, N=8, K=16, P_{FA0}=10^{-2}, 1st file.

Fig. 29 – Probability of false alarm with real HH data, N=8, K=16, P_{FA0}=10^{-1}, 1st file.
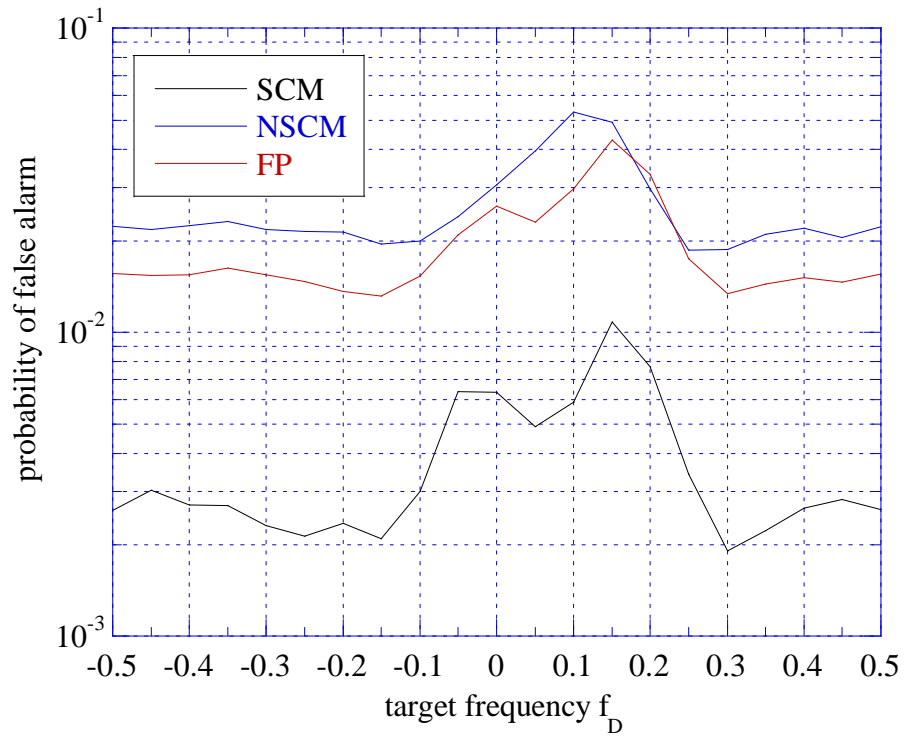

Fig. 30 – Probability of false alarm with real HH data, N=8, K=16, P_{FA0}=10^{-2}, 1st file.

The differences between nominal and actual P_{FA} are evident, particularly for $P_{FA0}=10^{-2}$. The actual P_{FA} of NAMF-NSCM and NAMF-FP are close to the nominal one only for f_D in the noise floor of the clutter. When f_D is close to the peak of the PSD, the real P_{FA} is higher than the nominal one, particularly for $P_{FA0}=10^{-2}$. On the contrary, the actual P_{FA} of the NAMF-SCM is almost always lower than the nominal one. The results are similar for both polarizations. It is important to observe that the deviations from the nominal value of the P_{FA} are higher in the area of the clutter spectrum in which the variations due to the non-stationarity of the clutter are greater. The variations of the noise floor are negligible. It is the peak of the PSD or the Doppler centroid that moves with the long waves originating the almost periodic behavior of the spectrogram as in Figs. 5-6.

The differences in the NAMF-SCM can be mostly due to the non-stationarity of the shape parameter of the K distribution to which the data belong, more than to the non-stationarity of the covariance matrix. The SCM is particularly sensitive to the clutter texture probability density function.

Obtaining a P_{FA} that is lower than the nominal one does not mean in general having a good result. The performance of the system depends also on the probability of detection. To evaluate it, we synthetically generated a Swerling I target, so that the data samples in the CUT have the following expression:

$$z(n) = \alpha \exp\left(j2\pi f_D n \right) + d(n) \tag{12}$$

for $n=0,1,\dots N-1$; α is a complex Gaussian random variable, i.e. $\alpha \in \mathcal{CN}\left(0,\sigma_\alpha^2\right)$, f_D is the Doppler frequency of the target and $d(n)$ is the clutter. The clutter-to-noise ratio (CNR) is defined as $SCR = \sigma_\alpha^2/\sigma_d^2$. In the simulation with synthetic clutter we set $\sigma_d^2 = 1$, in the test with real data the average power of the clutter has been estimated from the data as

$$\hat{\sigma}_d^2 = \frac{1}{N_c N_d} \sum_{k=1}^{N_c} \sum_{i=0}^{N_d-1} \left| z_k(n) \right|^2 \tag{13}$$

where N_c is the number of range cells and N_d the number of data per cell.

The results are summarized in the Figs. 31-34 for the 1st file, where we set $f_D=0$. It is evident from these figures that the performances of the three detectors are poorer with the real non-stationary data than with the simulated stationary clutter. The non-stationarity of the clutter influences also the probability of detection of the NAMF.

The performances of the NAMF for the 2nd file are summarized in Figs. 35-38. For a nominal $P_{FA0}=10^{-1}$ the estimated P_{FA} of NAMF-NSCM and NAMF-FP are pretty close to the theoretical one. This is not true for the NAMF-SCM that exhibits a P_{FA} lower than the nominal one. For $P_{FA0}=10^{-2}$ all the estimated P_{FA} are different from the nominal one. The results are similar for both polarizations. From Figs. 39-42, it appear evident that the actual P_D is always lower that the nominal P_D for each detector and matrix estimator.
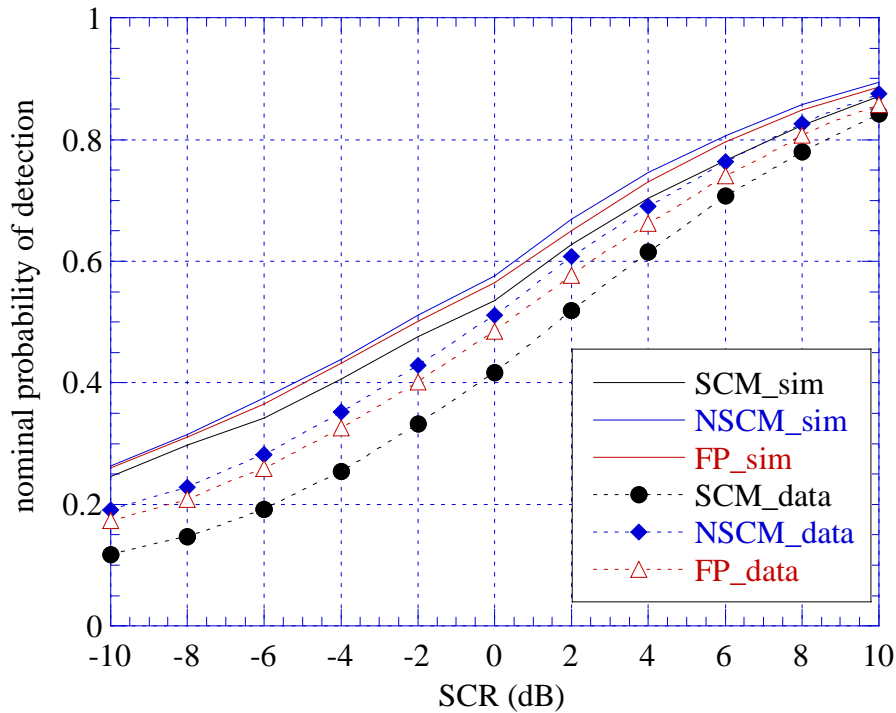

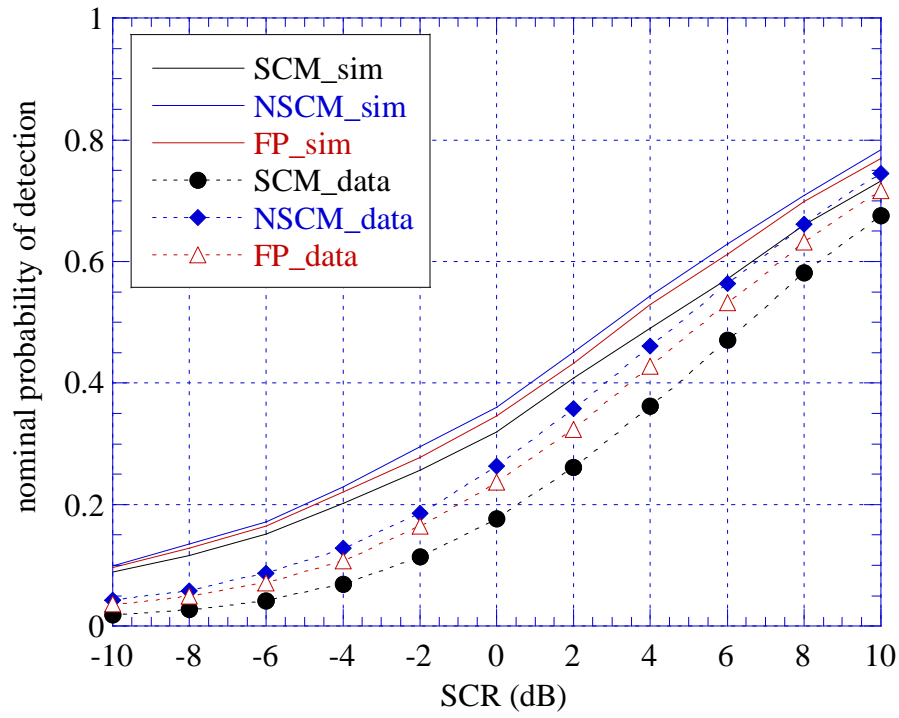**Fig. 31** – Probability of detection, $N=8$, $K=16$, $P_{FA0}=10^{-1}$, VV polarization, 1st file.

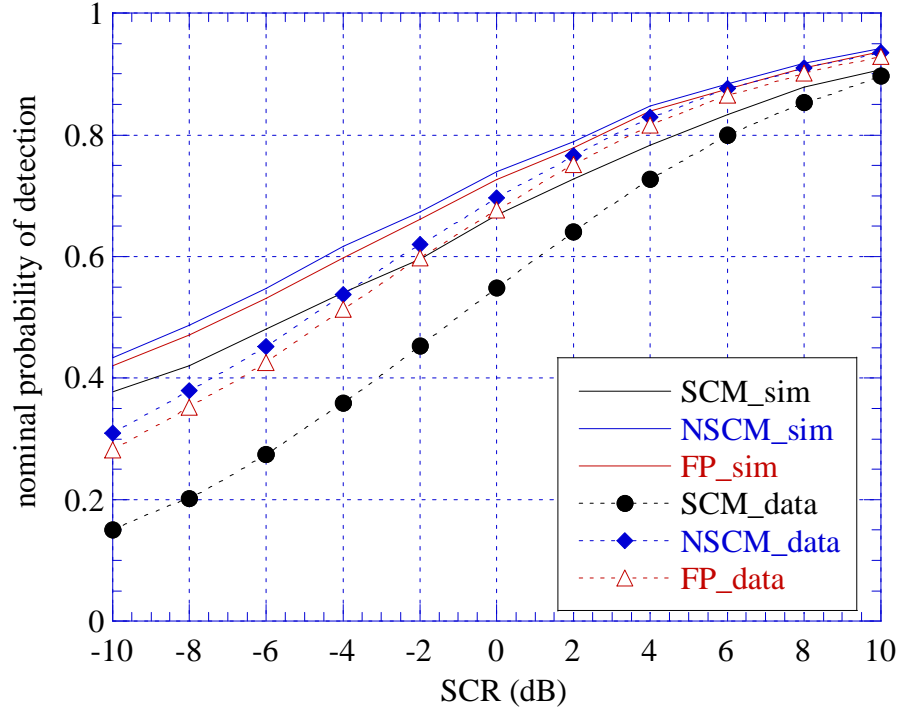**Fig. 32** – Probability of detection, N=8, K=16, P_{FA0}=10^{-2}, VV polarization, 1st file.

Fig. 33 – Probability of detection, N=8, K=16, P_{FA0}=10^{-1}, HH polarization, 1st file.
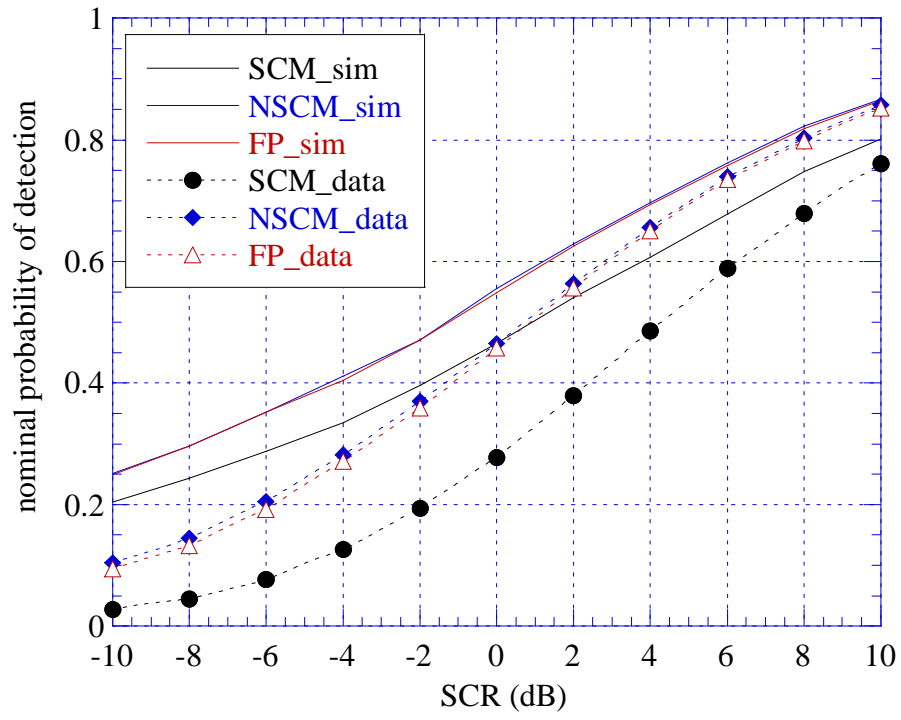
Fig. 34 – Probability of detection, $N=8$, $K=16$, $P_{FA0}=10^{-2}$, HH polarization, 1st file.
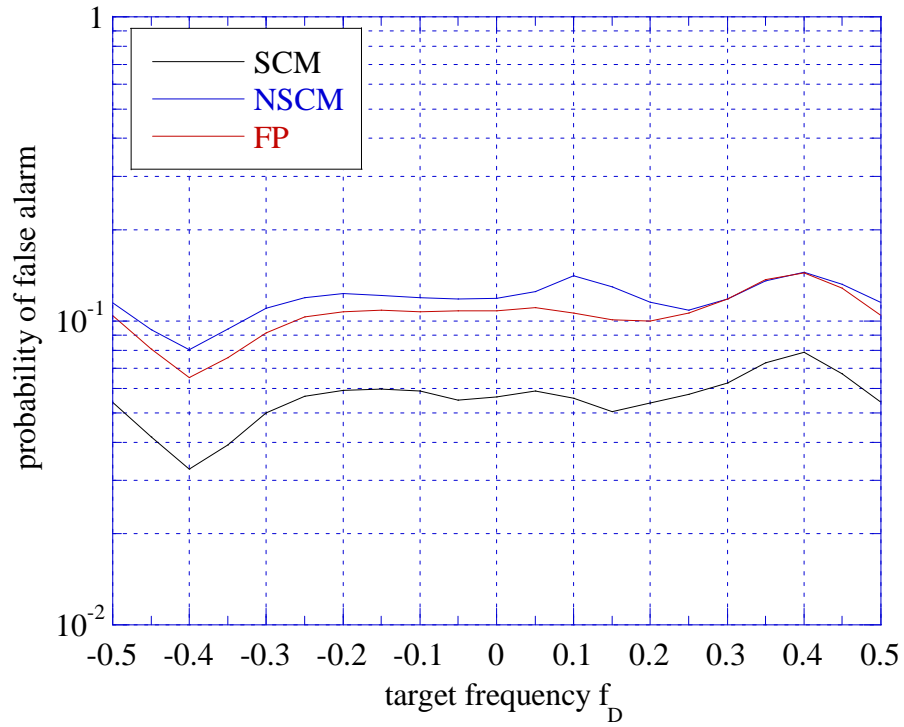

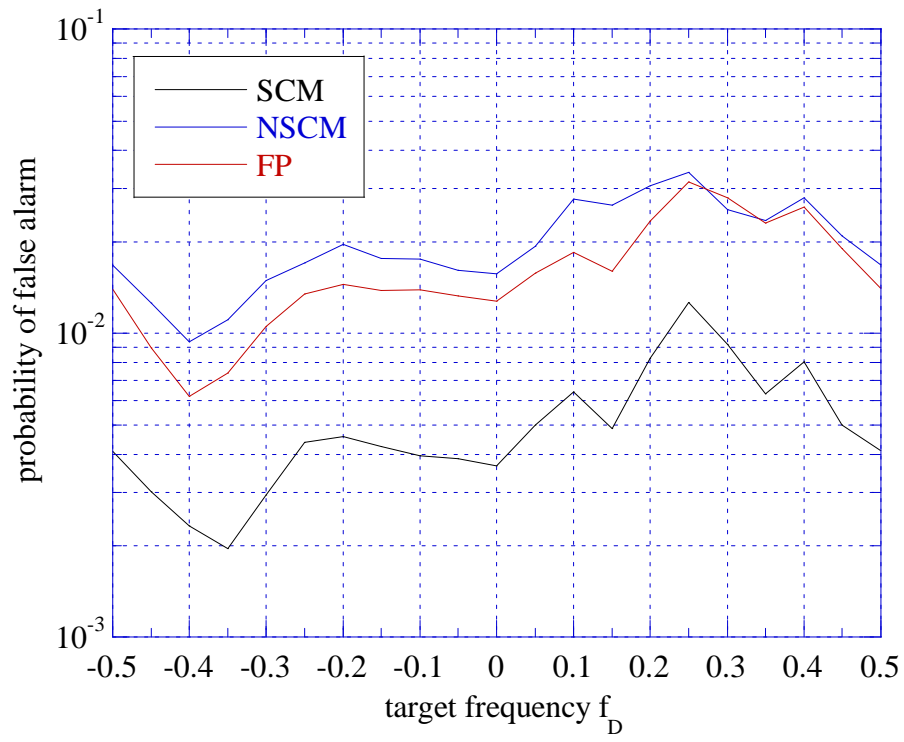**Fig. 35** – Probability of false alarm with real VV data, $N=8$, $K=16$, $P_{FA0}=10^{-1}$

Fig. 36 – Probability of false alarm with real VV data, N=8, K=16, P_{FA0}=10^{-2}
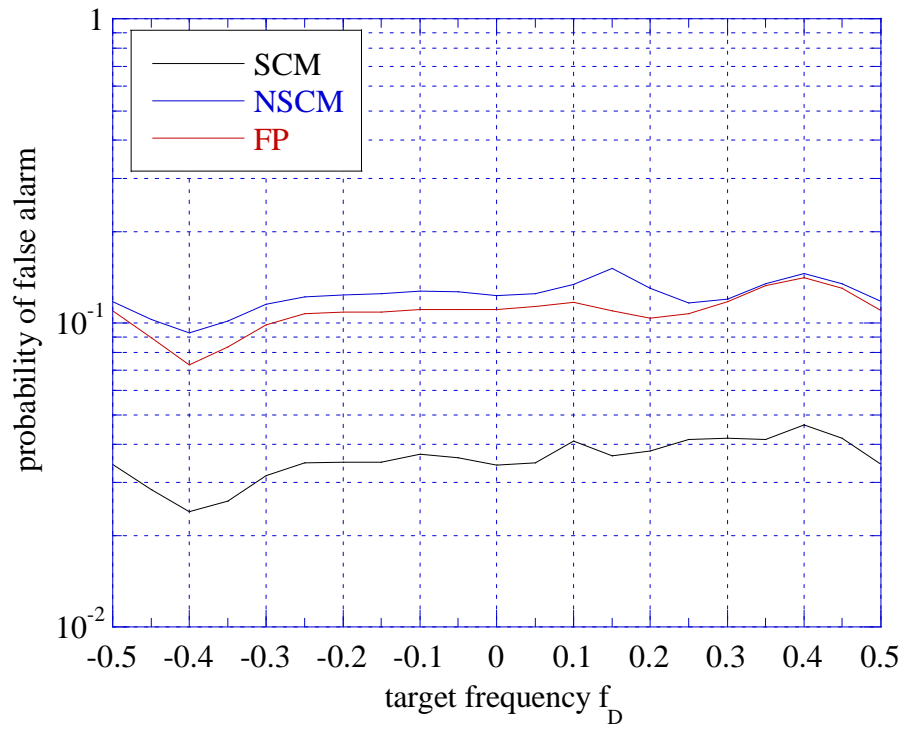

Fig. 37 – Probability of false alarm with real HH data, N=8, K=16, P_{FA0}=10^{-1}
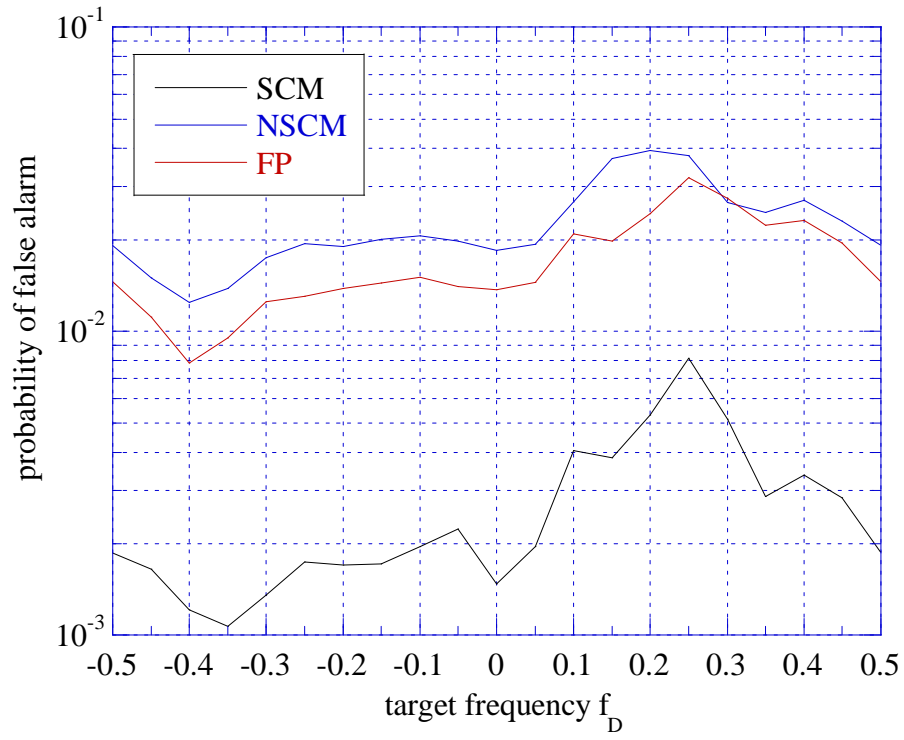
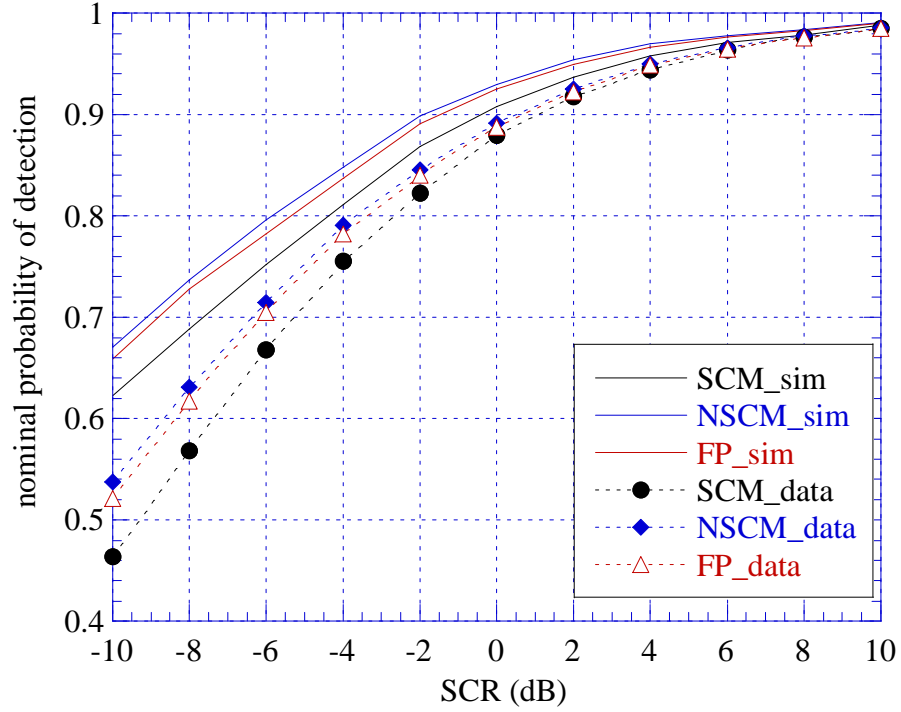**Fig. 38** – Probability of false alarm with real HH data, $N=8$, $K=16$, $P_{FA0}=10^{-2}$

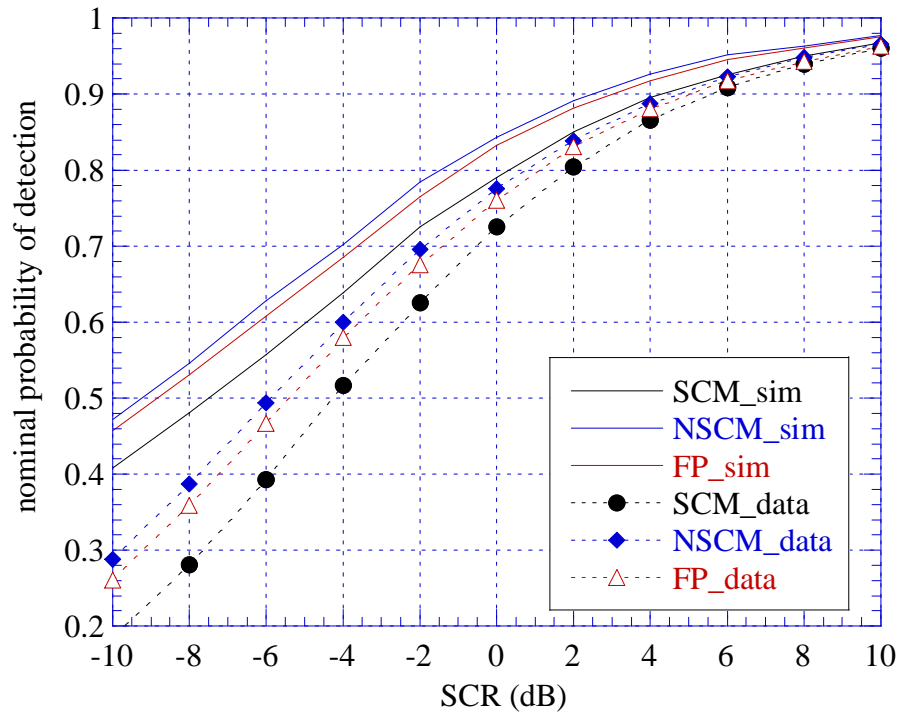**Fig. 39** – Probability of detection, $N=8$, $K=16$, $P_{FA0}=10^{-1}$, VV polarization.

Fig. 40 – Probability of detection, N=8, K=16, P_{FA0}=10^{-2}, VV polarization.
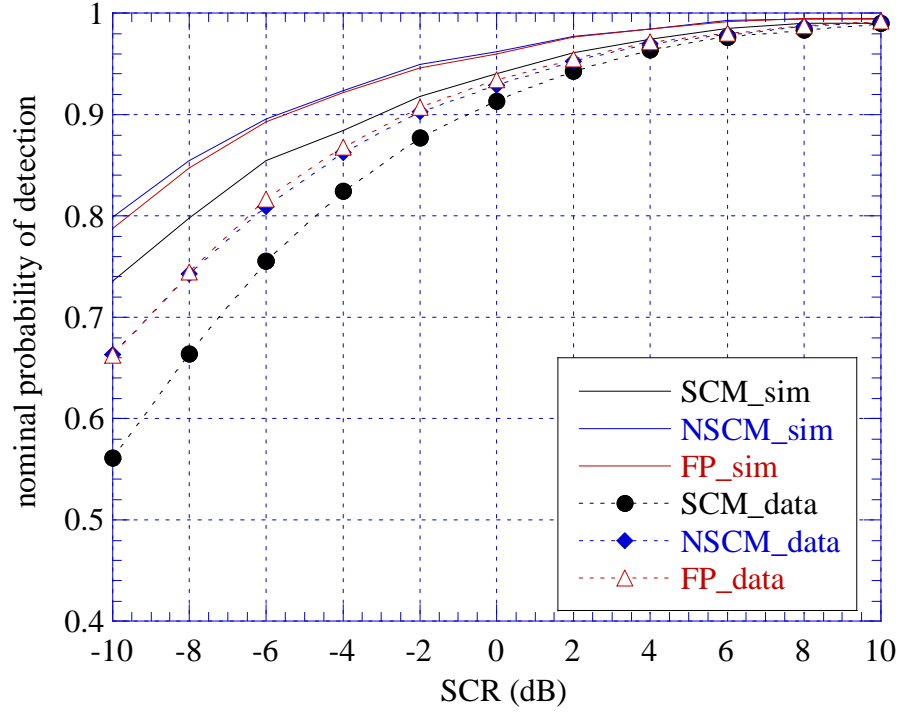

Fig. 41 – Probability of detection, N=8, K=16, P_{FA0}=10^{-1}, HH polarization.
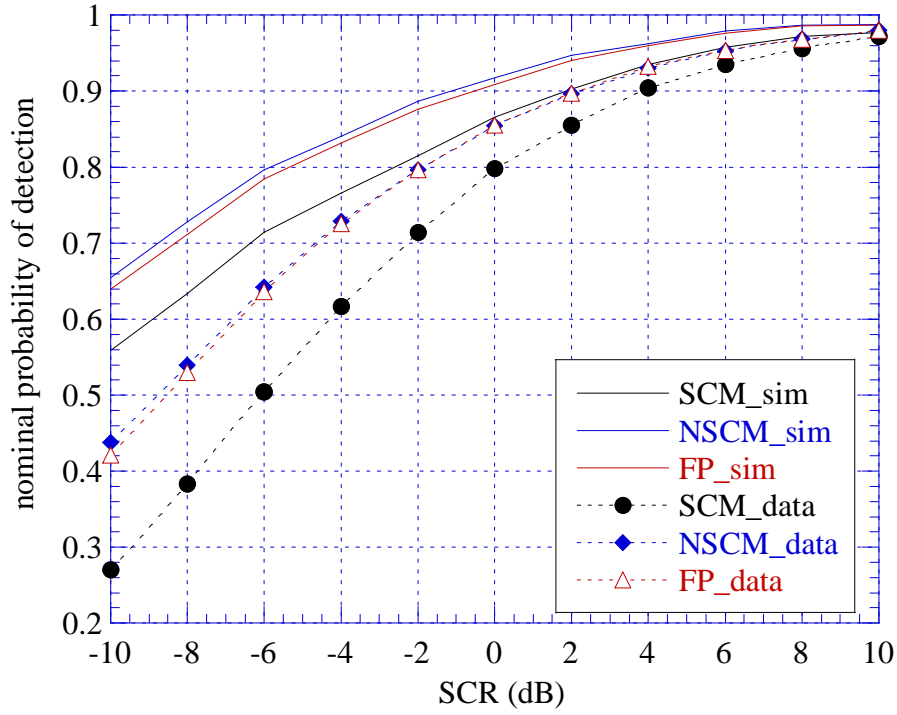
Fig. 42 – Probability of detection, $N=8$, $K=16$, $P_{FA0}=10^{-2}$, HH polarization.

We continued our analysis testing the NAMF 19980227_213808_antstep file data. In this file the range resolution is 15 m. The P_{FA} and the P_D are plotted in Figs. 43-50. Surprisingly, the probability of detection for the VV data is pretty close to the nominal one. The only difference with the other data is that this VV polarized clutter is less spiky than the others in the other two files. We can guess that the non-stationarity have a greater weight with spikier data. As a matter of fact, the P_D on the HH data shows same behaviour than in the previously analyzed files.

Fig. 43 – Probability of false alarm with real VV data, N=8, K=16, P_{FA0}=10^{-1}
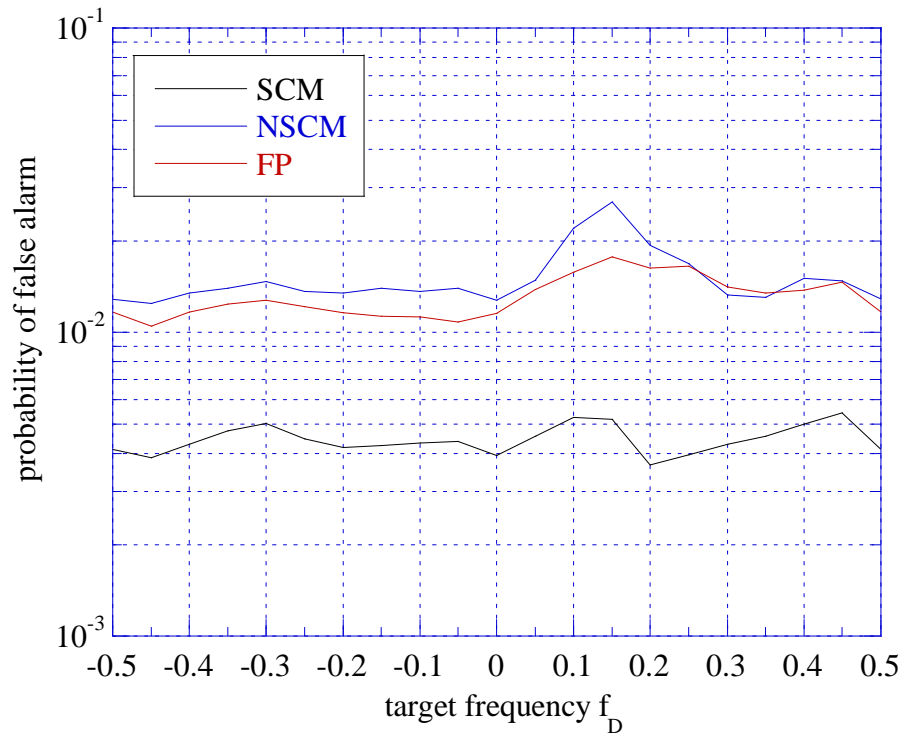
Fig. 44 – Probability of false alarm with real VV data, N=8, K=16, P_{FA0}=10^{-2}
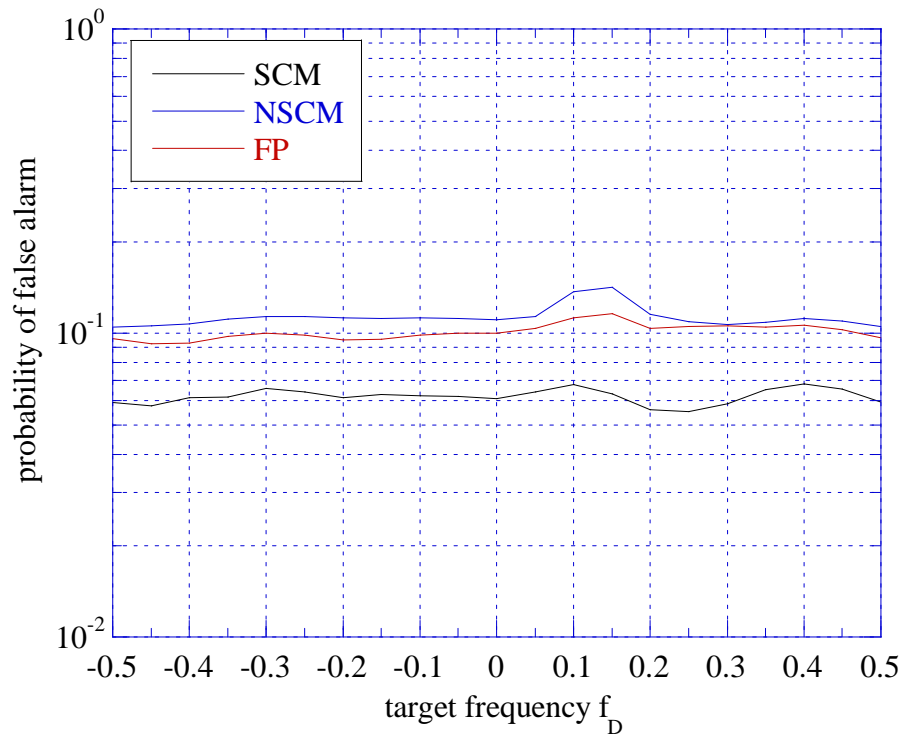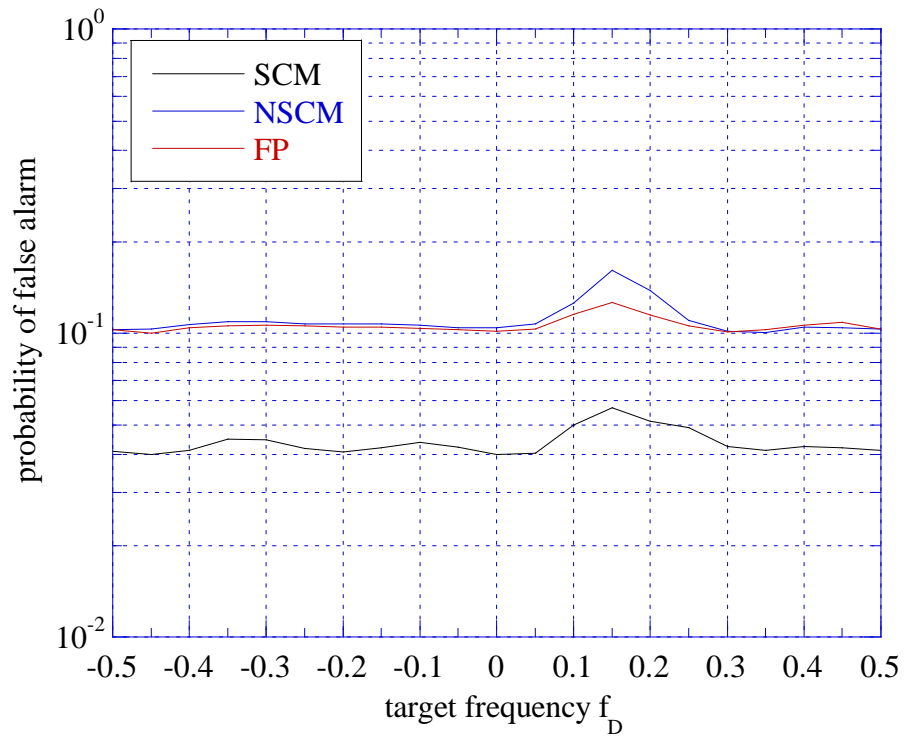
Fig. 45 – Probability of false alarm with real HH data, N=8, K=16, P_{FA0}=10^{-1}
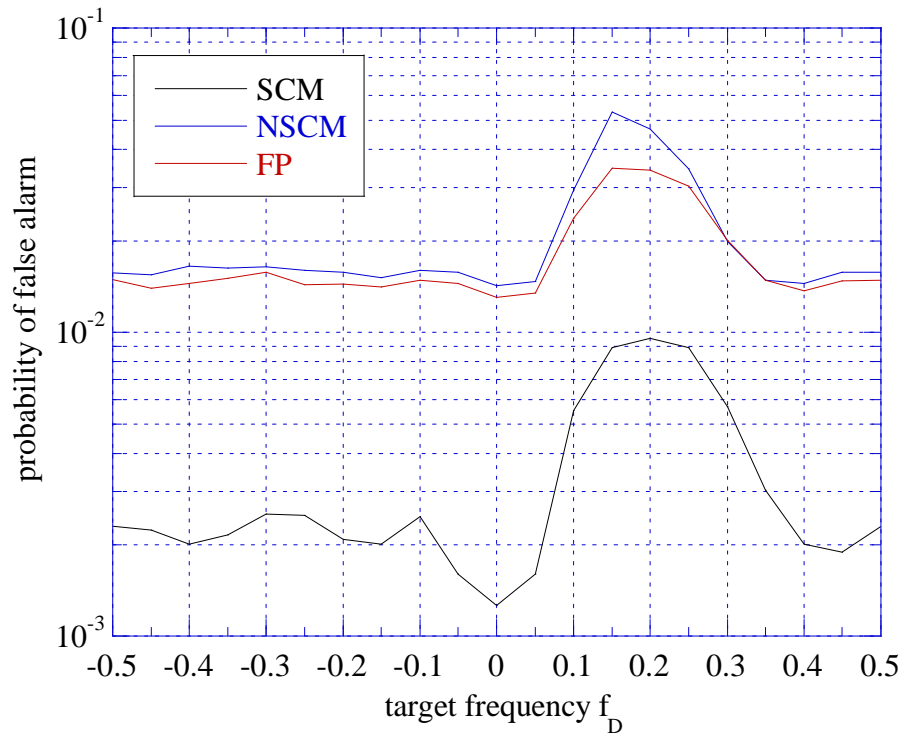
Fig. 46 – Probability of false alarm with real HH data, N=8, K=16, P_{FA0}=10^{-2}
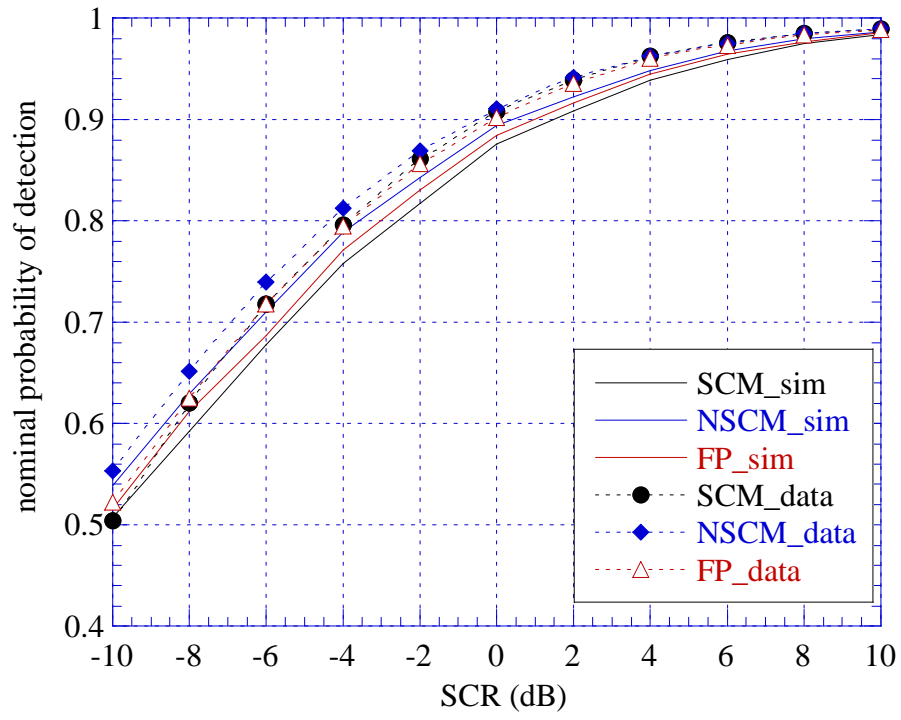
Fig. 47 – Probability of detection, N=8, K=16, P_{FA0}=10^{-1}, VV polarization.

Fig. 48 – Probability of detection, N=8, K=16, P_{FA0}=10^{-2}, VV polarization.

Fig. 49 – Probability of detection, N=8, K=16, P_{FA0}=10^{-1}, HH polarization.

Fig. 50 – Probability of detection, N=8, K=16, P_{FA0}=10^{-2}, HH polarization.

7. Conclusions

In this technical report we have analyzed HH and VV polarized lake clutter data and we have used them to test the performance of the Normalized Adaptive Matched Filter (NAMF) detector with the goal of verifying the imp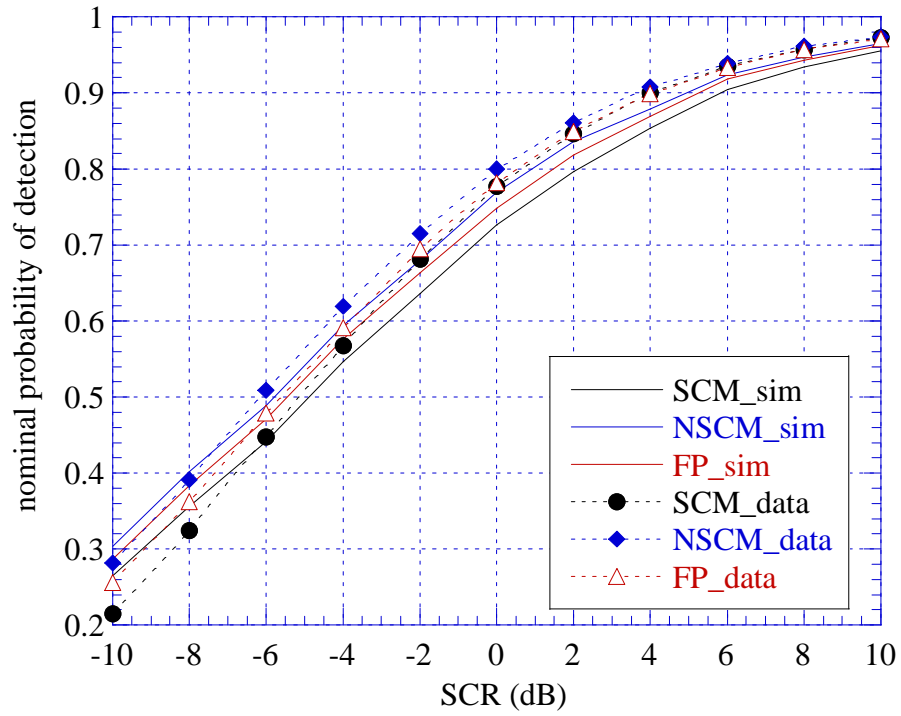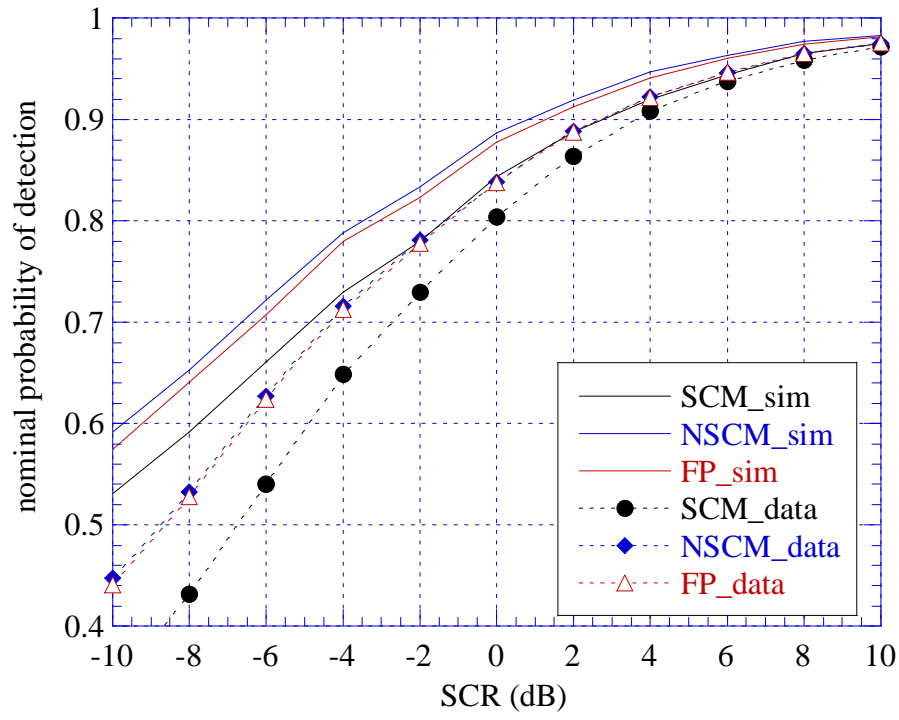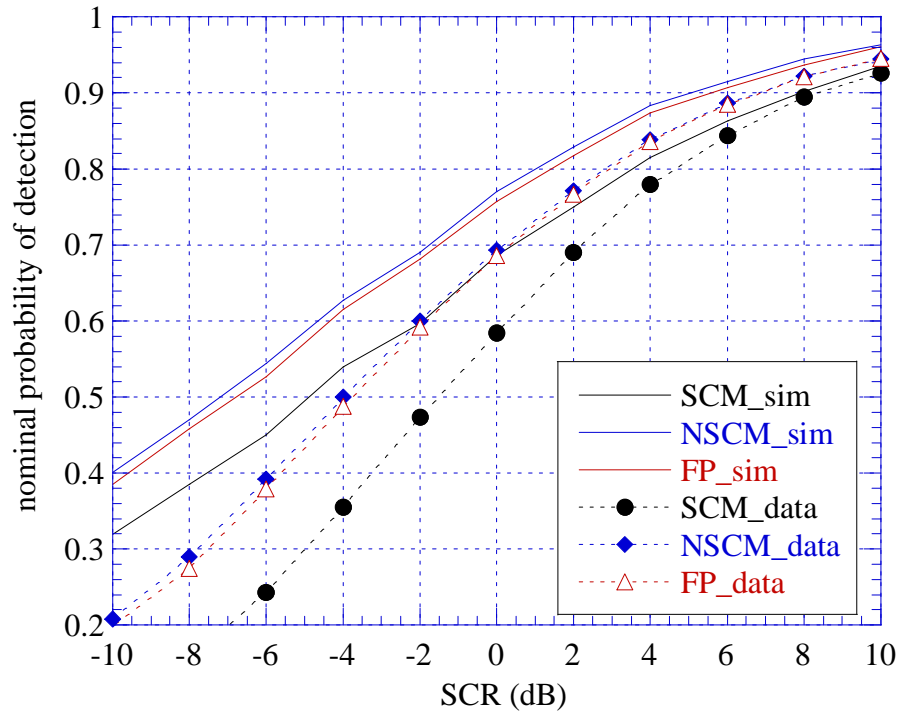act of temporal and spatial non-stationarity on the detector False Alarm Rate (FAR) and in general on the performance of the NAMF adopting different clutter covariance estimators. We applied the sample covariance matrix (SCM), the normalized sample covariance matrix (NSCM), and the fixed point (FP) matrix estimators. All the known properties of NAMF-SCM, NAMF-NSCM and NAMF-FP are based on the assumption that the clutter in the primary and secondary vectors shares same statistical properties, that is, the clutter is stationary in time and space. In real sea clutter scenario, unfortunately, often this is not the case. Our statistical analysis shows that:

1) The sea clutter show a good fit to K model but the shape parameter of the distribution changes from cell to cell.

2) The speckle PSD is no-constant in time and space, so the clutter is not spatially and temporally stationary. The spectrogram evidences some temporal periodicity in spectrum PSD behavior.

To measure the impact of clutter non-stationarity on CFAR property of the NAMF, we generated a K clutter with a covariance matrix equal to the average covariance matrix of the real data and with a shape parameter equal to the estimated v_{mean}. We performed a thorough numerical analysis by processing these simulated data, for different values of the target Doppler frequency f_D, and we set the threshold for a nominal probability of false alarm $P_{FA0} = 10^{-1}$ and $P_{FA0} = 10^{-2}$.

After setting the nominal thresholds we estimated the probability of false alarm and of detection of the NAMF fed by the real data. If the data had same statistical properties of the simulated data, the performance of the NAMF with real data and with simulated data would be very close. Conversely, in our results we observed large differences in the P_{FA} and in the P_D, almost always. Most of these differences can be attributed to the spatial and temporal non-stationarity of real data that can imply a variation of the P_{FA} of one order of magnitude with respect to the nominal one, and of the SCR for a fixed P_D of 2-5 dB. The impact of the nonstationarity seems to be stronger and stronger with increasing spikiness and decreasing P_{FA}.

References

[Bau07] S. Bausson, F. Pascal, P. Forster, J.-P. Ovarlez, P. Larzabal, "First- and second-order moments of the normalized sample covariance matrix of spherically invariant random vectors", *IEEE Signal processing Letters*, Vol. 14, No. 6, June 2007, pp. 425-428.

[Con94] E. Conte and G. Ricci, "Performance prediction in compound-Gaussian clutter", *IEEE Transactions on Aerospace and Electronic System*, vol. 30, pp.611-616, April 1994.

[Con95] E. Conte, M. Lops, G. Ricci, "Asymptotically optimum radar detection in compound-Gaussian clutter", *IEEE Transactions on Aerospace and Electronic Systems*, vol. 31, no. 2, pp. 617-625, April 1995.

[Con02a] E. Conte, A. De Maio and G. Ricci, "Covariance matrix estimation for adaptive CFAR detection in compound-Gaussian clutter", *IEEE Transactions on Aerospace and Electronic Systems*, vol. 38, No.2, pp.415-426, April 2002.

[Con02b] E. Conte, A. Demaio and C. Galdi, "Statistical analysis of real clutter at different range resolutions", *IEEE Transactions on Aerospace and Electronic System*, vol. 40, No. 3, pp.903-918, July 2002.

[Con02c] E. Conte, A. De Maio and G. Ricci, "Recursive estimation of the Covariance matrix of a compound-Gaussian clutter and its application to adaptive CFAR detection", *IEEE Transactions on Signal Processing*, Vol. 50, No.8, August 2002.

[Far97] A. Farina, F. Gini, M. V. Greco, L. Verrazzani, "High resolution sea clutter data: a statistical analysis of recorded live data", *IEE Proc.-Radar, Sonar and Navigation*, vol.144, no. 3, pp-121-130, June 1997.

[Ger02] K.R. Gerlach, "Outlier resistant adaptive matched filtering", *IEEE Transactions on Aerospace and Electronic Systems*, vol. 38, no. 1, pp.885-901, 2002.

[Gin97] F.Gini, "Sub-optimum coherent radar detection in a mixture of K-distributed clutter and Gaussian clutter", *IEE Proc.-Radar, Sonar and Navigation*, February 1997, pp. 39-48.

[Gin99] F. Gini, J.H. Michels, "Performance analysis of two covariance matrix estimators in compound-Gaussian clutter", *IEE Proceedings -Radar, Sonar and Navigation*, Vol. 146, No. 3, June 1999, pp. 133-140.

[Gin02]   F. Gini, M. Greco, "Covariance matrix estimation for CFAR detection in heavy clutter", *Signal Processing*, vol. 82, pp. 1495-1507, 2002.

[Gin06]   F. Gini, M. Greco, and M. Rangaswamy, "*Statistical Analysis of lake clutter data with different wind directions*", Contract FA8655-06-1-30100, University of Pisa, Italy, September 2006.

[Gre04]   M. Greco, F. Bordoni, F. Gini, "X-band Sea Clutter Non-Stationarity: The influence of Long Waves," *IEEE Journal on Ocean Engineering*, Special Issue on "Non-Rayleigh Reverberation and Clutter", special issue, Vol.29, No. 2, April 2004, pp.269-283.

[Gre06]   M. Greco, F. Gini and M. Rangaswamy, "Statistical analysis of measured polarimetric clutter data at different range resolutions", *IEE Proceedings, Radar, Sonar and Navigation*, Vol. 153, No. 6, pp. 473-481, December 2006.

[Hay02]   Haykin S., Bakker R., Currie B.W., "Uncovering Nonlinear Dynamics - The Case Study of Sea Clutter," *Proceedings of the IEEE*, Vol. 90, No. 5 , pp. 860 - 881, May 2002.

[Him98]   B. Himed, W. L. Melvin, "Analyzing space-time adaptive processors using measured data", in *Proc. of the 31st Asilomar conference on signals, systems and computers*, 1998, pp. 930-935.

[Kel86]   E. J. Kelly, "An adaptive detection algorithm", *IEEE Transactions on Aerospace and Electronic Systems*, vol. 23, pp. 115-127, Nov. 1986.

[Kra05]   S. Kraut, L. L, Sharf and R. W. Butter, "The adaptive coherence estimator: A uniformly most-powerful-invariant adaptive detection statistic", *IEEE Transactions on Signal Processing*, vol. 53, N. 2, pp. 427-438, Feb. 2005.

[Mel96]   W. L. Melvin, M. C. Wicks, and R. D. Brown, "Assessment of multichannel airborne radar measurements for analysis and design of space time adaptive processing architectures and algorithms", in *Proc. IEEE National Radar Conference*, Ann Arbour, MI, 1996.

[Mel97]   W. L. Melvin, M. C. Wicks, "Improving practical space-time-adaptive radar", in *Proc. IEEE National Radar Conference*, Syracuse, NY, 1997.

[Pas07]   F. Pascal, Y. Chitour, J. P. Ovarlez, P. Forster and P. Larbazal, "Covariance structure maximum likelihood estimates in compound Gaussian noise: existence and algorithm analysis", *IEEE Transactions on Signal Processing,* 2007, in press.

[Ran04]   M. Rangaswamy, J. H. Michels, and B. Himed, "Statistical analysis of the non-homogeneity detector for STAP applications", *Digital Signal Processing*, vol. 14, no. 3, pp. 253-267, 2004.

[Ran05]   M. Rangaswamy, "Statistical analysis of the non-homogeneity detector for non-Gaussian interference backgrounds", *IEEE Transactions on Signal Processing*, vol. 53, No. 6, pp. 2101-2111, June 2005.

[Ric96]   C.D. Richmond, "A note on non-Gaussian adaptive array detection and signal parameter estimation", *IEEE signal Processing Letters*, 1996, Vol. 3, No. 8, pp. 251-252.

[Kra05]   S. Kraut, L.L. Scharf, R.W. Buther, "The adaptive coherence estimator: a uniformly most-powerful-invarinat adaptive detection statistic", *IEEE Transactions on Signal Processing*, vol. 53, No. 2, pp. 427-438, February 2005.

[War94]   J.Ward, "Space time adaptive processing for air-born radar", Lincoln Laboratory Technical Report 1015, December, 1994.